**Title**
The Hidden Costs of Housing Practices: the importance of murine cold-stress to science



**Author**
David, John M.

**Publication Date**
2014

Peer reviewed|Thesis/dissertation

UNIVERSITY OF CALIFORNNIA

Los Angeles

# The Hidden Costs of Housing Practices:

# the importance of murine cold-stress to science

A dissertation submitted in partial satisfaction of the

requirements for the degree Doctor of Philosophy

in Molecular and Medical Pharmacology

by

John M David

2014

The dissertation of John M David is approved.

_____

Harvey R Herschman

_____

Lily Wu

_____

Nigel T Maidment

_____

Kenneth P Roos

_____

Arion-Xenofon Hadjioannou, Co-Chair

_____

David B Stout, Co-Chair

University of California, Los Angeles

2014

ABSTRACT OF THE DISSERTATION

The Hidden Costs of Housing Practices:

the importance of murine cold-stress to science

By

John M David

Doctor of Philosophy in Molecular and Medical Pharmacology

University of California, 2014

David B Stout, Co-Chair

Arion-Xenofon Hadjioannou, Co-Chair

Laboratory mice housed in modern vivariums are chronically cold-stressed. Cold-stressed mice exhibit compensatory non-shivering thermogenesis that drives a significant increase in total energy expenditure. In this manuscript, we will describe the visualization and quantification of non-shivering thermogenesis with thermography as a metric of murine cold-stress (Chapter 2). Utilizing thermography to measure cold-stress within the vivarium, we will show mice housed in individually ventilated caging, a popular and important housing system, exhibit significantly greater non-shivering thermogenesis than mice housed in static cages. Xenograft tumors implanted in mice housed in individually ventilated cages have blunted growth and metabolism compared to static cages. The experimental variability between housing systems can be significantly, but incompletely, mitigated by the addition of shelters that allow mice to maintain heated micro-climates (Chapter 3). Housing dependent variations in experimental results is likely a confounder throughout murine dependent research. We

designed and validated novel ventilated caging designed to minimize the chilling effects of individually ventilated cages while preserving the benefits of ventilated caging (Chapter 4).

## DEDICATION

This work is a testament of my mentors' unwavering efforts and devotion to education. I dedicate the work with deep respect and gratitude to these extraordinary people: David Stout, Gregory ("G") Lawson, Marcelo Couto, Sandra Vogel Duarte, Lisa Williams, and Scott Hunter.

Thank you.

To my family, thank you for your steadfast support, love, and tenacity through this long journey. I especially recognize the following family members: Cat and Axelle Watkins-David, Henry, Charissa, Cecily, Ally, and Max David, and Joan Collins-Lund.

Much love to all of you.

## TABLE OF CONTENTS

**PAGE**

## LIST OF FIGURES

## LIST OF TABLES

## LIST OF SYMBOLS AND ACRONYMS

| | |
|---|---|
| $^{18}F$ | Fluoride radio-isotope |
| $^{18}F$-FDG | $^{18}F$-Flurodoxyglucose |
| ΔT BAT | Emitted heat of brown adipose region above an internal control region |
| ε | Emissivity |
| ACH | Air changes per hour |
| AMIDE | A medical image data examiner software |
| BAT | Brown adipose tissue |
| Bq | Becquerel |
| $CO_2$ | Carbon dioxide |
| EPR | Entropy production rate (calorie per minute) |
| ID% | Injected dose percent |
| LCT | Lower critical limit |
| m/s | meters/second |
| $NH_3$ | Ammonia |
| $O_2$ | Oxygen |
| PET | Positron emission tomography |
| ppm | Parts per million |

| | |
|---|---|
| $R^2$ | Coefficient of determination calculation |
| RQ | Respiratory quotient ($VCO_2/O_2$) |
| ROI | Region of interest |
| SUV | Standard uptake value |
| TNZ | Thermal neutral zone |
| UPC1 | Uncoupling protein 1 |
| WAT | White adipose tissue |

## ACKNOWLEDGMENTS

To David Stout for providing daily guidance on science, preclinical imaging, management, regulations, graduate school, and life. David has been and continues to be an remarkable teacher and friend.

To Waldemar Ladno and Darin Williams for teaching me about the day-to-day operation of the Crump Preclinical Imaging Technology Center and Solid Works.

To my committee members, Drs. Harvery Herschman, Lily Wu, Nigel Maidment, Kenneth Roos, Arion Hadijoannou, and David Stout, for your support and candor through the training process. Your high standards and enthusiasm for science makes UCLA a special place.

To Drs. Arion Hadjioannou, Hongkai Wang, Richard Taschereau, and Scott Knowles for the training and consulting on medical imaging.

To the Division of Laboratory Animal Medicine family: thank you for your kindness, opportunity to train at a world-class research facility, and learn from your collective wisdom. Your work and dedication to the animals and the science is making positive impact on the world.

To the Dean's Office 3Rs and Crump family for your generous support of this work.

Finally, I am using this space to acknowledge and appreciate the animals. They have taught us much about the world and ourselves.

Chapter 2 is adapted from the following works:

1. David JM, Chatziioannou A, Taschereau R, Wang H, Stout DB. 2013. Quantifying chronic cold-stress of laboratory rodents with non-invasive imaging. Comp Med, 63(5): 386-91.
2. David JM, Stout DB. 2013. Poster: Quantifying Cold-stress in Laboratory Mice with Thermography: a non-invasive imaging technique. Am Ass for Lab An Sci, Baltimore, MD.

Chapter 3 is adapted from the following works:

1. David JM, Knowles S, Lamkin D, Stout DB. 2013. Individually Ventilated Cage Impose Cold-stress on Laboratory Mice: a source of experimental variability. J Am Assoc Lab Anim Sci, 52(6): 738-44.
2. David JM, Stout DB. 2013. Presentation: Individually Ventilated Cages, an Experimental Confounder. AALAS, Baltimore, MD.

Figure 1.1 has been adapted from the following manuscript with permission:

Cannon B, Nedergaard J. 2010. Nonshivering thermogenesis and its adequate measurement in metabolic studies. J of Exp Bio 214: 242-53.

Figure 1.2 has been adapted from the following manuscript with permission:

Gaskill BN, Gordon CJ, Rajor EA, Lucas JR, Davis JK, Garner GP. 2012. Heat or Insulation: behavioral titration of mouse preference for warmth or access to a nest. PloS one 7(3): e32799.

Figure 1.2 has been adapted from the following manuscript with permission:

Gordon CJ. 2012. Thermal physiology of laboratory mice: defining thermoneutrality. J of Thermal Bio 37(8): 654-685.

Figure 3.2 has been adapted from the following manuscript with permission:

Chappell MA, Holsclaw DS. 1984. Effects of wind on thermoregulation and energy balance in deer mice (*Peromyscus maniculatus*). J Comp Physiol B 154: 619-625.

## VITA

| | |
|---|---|
| 2003-2005 | Animal Behavior Intern, UC Davis |
| 2001-2005 | Davis Honors Challenge, UC Davis |
| 2005 | B.S. in Animal Biotechnology, UC Davis |
| 2008 | Veterinary Pathology Student Scholarship, CL Davis Foundation |
| 2008 | Certified in basic micro-surgery, Loma Linda University |
| 2009 | Eli Lily Veterinary Externship Award, Eli Lilly and Company |
| 2009 | Doctor of Veterinary Medicine, Western University of Health Sciences |
| 2009 | Licensed by the California Veterinary Medical Board |
| 2009-2011 | Veterinary Resident, David Geffen School of Medicine, UCLA |
| 2012-2013 | 3Rs Grant, Role: PI, Dean's Office, David Geffen School of Medicine, UCLA |
| 2013 | Diplomat of the American College of Laboratory Animal Medicine |

## PATENTS, PUBLICATIONS, AND PRESENTATIONS

**David JM**, Irizarry. 2008. Using a literature mining resource to accelerate student-centered learning in a veterinary PBL curriculum. J of Vet Medical Education, Vol 36 (2), 202-208.

**David JM**, Dick, and Hubbard. 2009. Spontaneous pathology of the common marmoset (Callithrix jacchus) and tamarins (Saguinus oedipus, S. mystax). J Med Primatol 38 (5), 347-59.

**David JM,** Lawson G. 2010. Poster: Clinical Presentation of a Breeding Line of Stem Cell Cassette Lentivirus-loxP Male Mice with Multiple Round Cell Cutaneous Neoplasia; AALAS.

**David JM**, Berry-Pusey B, Chatziioannou A, Stout DB. 2012. Presentation: Irreproducibility of

Lateral Vein Injections: a case for using technicians' skills in laboratory settings. AALAS.

**David JM**, Knowles S, Taschereau R, Chatiioannou A, David S. 2013. Poster: Murine brown fat metabolism measured by thermography correlated with PET $^{18}$F-FDG uptake. Soc of Nuc Med and Mol Imaging.

**David JM**, Stout DB. 2013. Poster: Quantifying Cold-stress in Laboratory Mice with Thermography: a non-invasive imaging technique. AALAS.

**David JM**, Stout DB. 2013. Presentation: Individually ventilated cages, an experimental confounder. AALAS.

Berry-Pusey BN, Chang YC, Prince S, Chu K, **David JM**, Taschereau R, Silverman R, Williams D, Ladno W, Stout D, Tsao TC, Chatziioannou A. 2013. A semi-automated vascular access system for preclinical models. Phys in Med and Bio 58(16), 5351-62.

Xu J, Escamilla J, Mok S, **David JM**, Priceman S, West B, Bollage G, McBride W, Wu L. 2013. CSF1R signaling blockade stances tumor-infiltrating myeloid cells and improves the efficacy of radiotherapy in prostate cancer. Cancer Res*,* 73(9), 2782-94.

**David JM**, Knowles S, Lamkin D, Stout DB. 2013. Individually ventilated cage impose cold-stress on laboratory mice: a source of experimental variability. JAALAS, 52(6): 1-7.

**David JM,** Chatziioannou A, Taschereau R, Wang H, Stout DB. 2013. Quantifying chronic cold-stress of laboratory rodents with non-invasive imaging. Comp Med, 63(5): 386-91.

**David JM,** Stout DB. 2013. U.S. Patent No. 61/895,885 (provisional): System for reducing cold stress of housed laboratory animals. Washington, DC: Patent and Trademark Office.

Braga M, Reddy ST, Pervin S, Vernes L, Grijalva V, Stout DB, **David JM**, Li X, Tomasian V, Devaskar S, Reue K, Singh R. 2014. Follistatin promotes brown character of white adipocytes and influences energy metabolism. J Lipid Res, DOI 10.1194

Dick EJ, Owston MA, **David JM**, Sharp MS, Rouse S, Hubbard GB. 2014. Mortality in captive baboons (*Papio* spp.): A 23 Year Study. J Med Primatology, *in press*.

# Chapter 1: Introduction to the thermal biology of the mouse

## I. The modern laboratory mouse

In the post-genomic era, mice are the premier model of human disease, (Muller and Grossniklaus, 2010). A successful *in vivo* model requires two elements: translatability and reproducibility (Anon, 2009; Hutchinson, 2011). Governments, academic institutions, and private entities have spent vast resources on maintaining strict genomic definition of mice. Yet despite these investments, strict murine genomic definition still leaves room for great model variability because mice exhibit high phenotypic plasticity: variable phenotypes despite a fixed genome (Richter *et al.*, 2011). The key point of this work is the conditions of modern individually ventilated cages impose cold-stress on mice. The additional cold-stress associated with individually ventilated cages alters murine physiology, experimental reproducibility, and lead to the irreproducibility of murine experiments.

This work aims to explore housing driven phenotypic plasticity and to develop solutions to narrow the variation and to increase experimental reproducibility across housing systems. This chapter will provide background information on regulatory standards, murine physiological and behavioral response to cold, and relevance to experimental results. Because mice are key models in the fields of oncology, cardiovascular disease, metabolism and diabetes, regenerative medicine, genetics, and neurology (Muller and Grossniklaus, 2010), the topic of murine experimental reproducibility presented in this work has a broad range of impact to the scientific community.

## II. Thermal environment of the modern vivarium

The *Guide for the Care and Use of Laboratory Animals* (the "*Guide*"; NRC, 2011) sets the standards for domestic and international vivariums. The *Guide* serves as the basis of the National Institutes of Health's Office of Laboratory Animal Welfare Assurance and the Association for Assessment and Accreditation of Laboratory Animal Care, international accreditation. The *Guide* recommends a macro-environmental (room) temperature of 20°C to 26°C (68-79°F; NRC, 2011). In practice, most vivariums in the USA and abroad are maintained between 20-23ºC ("room temperature") for human comfort (Gaskill *et al.*, 2009).

## III. **Thermoneutrality**

The thermonetural zone (TNZ) is defined as a temperature range that an endotherm's heat production of resting metabolic rate is at equilibrium with heat loss to the surrounding environment (Cannon and Nedergaard, 2010). An endotherm's TNZ is determined by body size, morphology, insulation, and resting metabolic rate (Gordon, 2012). Within this zone, core body temperature is regulated by behaviors, peripheral vessel diameter, and body posture (see below; Gordon, 2012). The TNZ is bound by the lower critical (LCT) and upper critical limits; beyond these boundaries, endotherms engage active heating or cooling adaptations to maintain core body temperature. These thermal adaptations are energy intensive and drive increased metabolic rate (Figure 1-1; Cannon and Nedergaard, 2010).

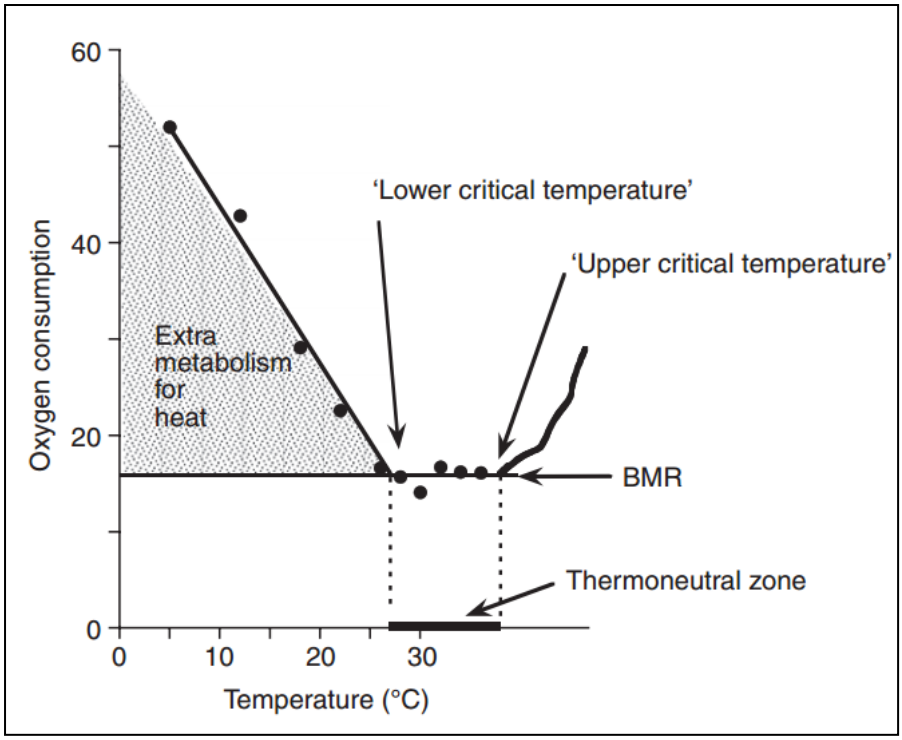


**Figure 1-1** The energetic consequence of different ambient temperatures. "Metabolism is fully governed by intrinsic factors only within a narrow zone of ambient temperatures- the thermoneutral zone (indicated by the area between the dashed lines, i.e. the lower and upper critical temperatures)." Within the thermoneutral range, the caloric expenditure of an organism is determined by the basal metabolic rate (BMR). "Oxygen consumption rates are arbitrary units." Beyond the lower and upper critical limits, endotherms actively heat and cool at great energetic costs. Reprinted from Cannon and Nedergaard (2011) with permission.

Laboratory mice are especially prone to cold-stress due to a large surface-to-volume ratio, poor insulation (Kaiyala, 2010; Scholander, 1950), and relatively narrow TNZ that typically spans 1 to 3°C (Gordon, 2012). The LCT for most laboratory mice ranges between 29 to 32°C. A handful of strains and life stages have notably lower LCT: e.g., obese OF1 mice (LCT 24.6ºC) and pregnant and lactating animals (Pennycuik, 1967; Gordon, 2012). Modulators of LCT are numerous and have been well summarized elsewhere (Figure 1-2; Gordon, 2012).

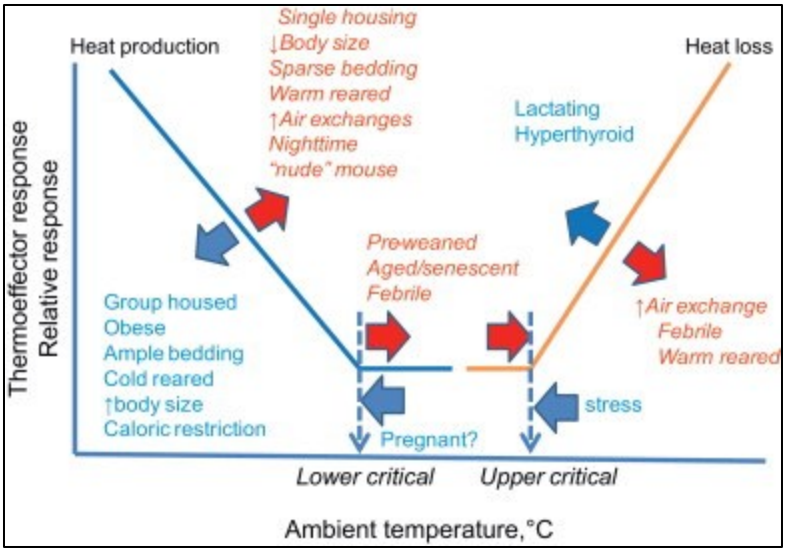


**Figure 1-2** Summary of modulators of the thermoeffective response. Parameters in blue are associated with cold resistance and preference with cooler temperatures. Parameters in red are associated with heat resistance and preference with warmer temperatures. Reprinted from Gordon (2012) with permission.

## IV. **Phenotypic plasticity**

The muriadiae family have been extraordinarily successfully living in a wide range of habitats, despite their small size and challenges with chronic cold-stress (Jacob *et al.*, 2002). The wide spread evolutionary success of mice is in part due to their phenotypic plasticity: exhibiting different phenotypes in response to environmental parameters in spite of a fixed genome. Mice exhibit a variety of thermal adaption to cold-environments. These adaptions vary in energy costs. Mice utilize these adaptations in the order of least to greatest energy costs (measured by oxygen consumption; see indirect calorimetry), always seeking to preserve energy (Gordon, 2012).

### a. **Behavioral thermoregulation**

Behavior is the first and preferred adaptation of mice (Gordon, 2012). Behavioral adaptations preceed physiological responses such as thermogensis (see thermogenesis below; Gordon, 2012). Behavioral thermoregulation centers around trapping metabolic heat locally to create heated micro-climates that are warmer than the surrounding environment (Gaskil, 2012; Gordon *et al.*, 1998). The three primary behavioral adaptations of mice are thermotaxis (seeking heat), nest building, and social huddling (Gaskil, 2012; Gordon, 1998). Behavioral thermoregulation is the less energetically intense compared to thermogenesis (further discussion below).

#### i. **Thermotaxis**

Thermotaxis is the locomotion towards a warmer environment. In time budget studies, mice spend most of their time in the warmest environment available (up to the upper critical limit; Gaskill *et al.*, 2009; Gaskill *et al.*, 2011). Thermal preferences are sensitive to circadian rhythm: during the light cycle, a period dominated by sedentary behaviors, mice prefer 30 to 32ºC; during the dark cycle, when physical activity peaks, mice select ambient temperatures of 26ºC; and the average selected temperatures over a 24 hour cycle ranges from 27.7 to 28.6ºC (Gordon, 1994; Gordon *et al.*, 1998; Leon *et al.*, 2010).

#### ii. **Nest building and shelter seeking**

Shelters and nests provide insulation and allow mice to behaviorally maintain heated micro-climates (Figure 1-3; Gaskill *et al.*, 2012). Nesting is also effective in

creating an insulative barrier around the animal that can be easily manipulated to create the desired thermal conditions (Gaskill *et al*., 2012).

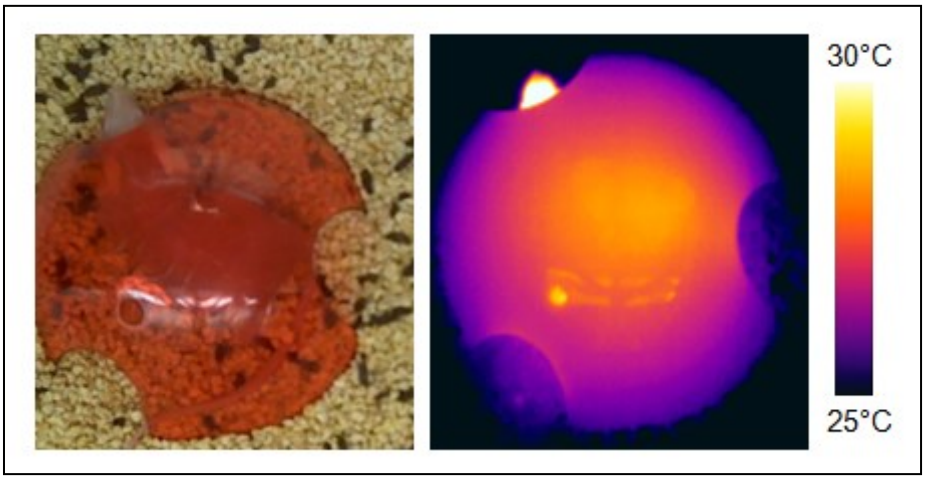


**Figure 1-3** Shelters augment behaviorally heated micro-climate. The dual photography (left) and thermal image (right) of a Nu-*Foxn1*$^{nu}$ mouse provided a shelters depicts a heated micro-climate within the shelter that is warmer than the surrounding cage environment.

Several investigators have observed welfare benefits from the addition of shelters and/or nesting materials to the cage: the addition of nesting material reduces food consumption without a corresponding decrease in body weight, suggesting a reduced energy demand (Olsson and Dahlborn, 2002). Gaskill observed a blunted thermotaxic response when mice were provided ample nesting materials (8-10 grams; Gaskill *et al*., 2012). These studies suggest cold-stress exists under routine housing conditions.

### iii. **Postural Changes**

When faced with a cold environments and/or drafts, mice will hunch, taking a spheroid shape and face the draft and erect their fur (piloerection), trapping a small pocket of insulating air around their body (Chappel and Holsclaw, 1984; Hammel,

1955). These postural changes reduce surface area and heat loss to environment (Chappel and Holsclaw, 1984).

iv. **Social Huddling**

Socially huddling, defined as “active and close aggregation of animals” (Gilbert *et al.*, 2010), is a well preserved thermoregulatory behavior seen in all small mammals and numerous avian species (Sealander, 1952). Groups of mice (“demes”) reduce their total surface area by ~35% (Batchelder *et al.*, 1982), maintain larger heated micro-climates than individual mice, increase group insulation, reduce feed consumption without loss of body weight, and reduce preferred ambient temperatures by ~1°C (Gaskill *et al.*, 2009; Gordon *et al.*, 1998). According to time budget studies, social huddling is the most common-and, by implication, the most important-social activity of mice (Arakawa *et al.*, 2007). Thus, it is likely the primary driver of social association of mice is thermal regulatory. Time spent in the huddle and size of the huddle increases in cooler environmental temperatures and vice versa (Batchelder *et al*., 1982; Heldmaier, 1975).

b. **Peripheral vasoconstriction**

The extremities represent the largest surface area-to-volume ratio of the mouse (Heldmaier, 1975). The majority of heat loss occurs via these peripheral sites. When cold, mice reduce peripheral blood flow to the tail and paws, dramatically lowering the heat loss to the environment and preserving heat in the core (Conley and Porter, 1985; Foster and Frydman, 1979).

Mice weaned in warmed in environments have longer tails than those in cold environments, which highlights the murine phenotypic plasticity and the importance of surface-area in thermal regulatory function (Al-Hili and Wright, 1983; Serrat *et al.*, 2008). However, the thermal thermoregulatory benefits of peripheral vasoconstriction are limited compared to larger species due to the mouse's small size and thin insulation (Philips and Heath, 1995). The thermal regulatory benefits of behaviorally mediated insulation (e.g. social huddling and nest building) are significantly greater than peripheral vasoconstriction (Grodon, 2012).

### c. **Thermogenesis**

When low energy adaptations are overwhelmed, endotherms increase metabolic heat production via thermogenesis: the physiological process of generating additional heat above basal metabolic rates utilizing stored chemical energy (IUPS Thermal Commission, 2001). Thermogenesis is an energetically intensive process and mice avoid it when possible (Gordon, 2012). Thermogenesis is divided into two sub-types: shivering and non-shivering.

#### i. **Shivering thermogenesis**

Shivering thermogenesis is the product of rhythmic contraction and relaxation of skeletal muscle. Shivering thermogenesis plays an important thermal regulatory role in larger, adult mammals, but is rarely utilized by mice who favor non-shivering thermogenesis (Oufara *et al.*, 1987). Adult mice will only use shivering thermogenesis when abruptly exposed to extreme cold; even then, the small muscle mass makes

shivering thermogenesis ineffective and mortality rates are high when mice are abruptly exposed to 4°C (Lim *et al.*, 2012).

### ii. **Non-shivering thermogenesis**

Neonatal and adult small rodent core body temperatures are dependent on non-shivering thermogenesis, which takes place in a specialized tissue called brown adipose tissue (BAT, also known as brown fat or, the historical misnomer, the hibernating gland; Ootsuka *et al.*, 2009; Krinke, 2004). BAT is rich in mitochondria with a high capacity for oxidative phosphorylation and beta-oxidation lipolysis (Celi, 2009; Schulz and Tseng, 2013). BAT contains a high concentrations of uncoupling protein 1 (UPC1), a mitochondrial inner membrane protein that dissipates the proton gradient generated from oxidative phosphorylation of nutrients (Schulz and Tseng, 2013). By discharging the proton gradient, UCP1 increases the rate of entropy, generating heat, at the expense of workable energy (Schulz and Tseng, 2013).

BAT is embryonically derived from *Myf5* positive myogenic lineage of mesodermal tissue, sharing a common progenitor cell with skeletal muscle (Seal *et al.*, 2008). Anatomically, the largest deposit of BAT is located in the intra-scapular region (iBAT). Smaller deposits are located adjacent to sympathetic ganglions, highlighting the close ties between BAT and the sympathetic nervous system (Thornhil and Halvorson, 1990). Some investigators have proposed this close physical relationship allows BAT mediated non-shivering thermogenesis to preserve the essential sympathetic neuron functions during life-threatening cold exposure (Thornhil and Halvorson, 1990).

Non-shivering thermogenesis is under the control of thyroid hormone (which can be locally converted from the low activity T3 form to the active T4 form), α1 and β3 adrenergic receptors (Celi, 2009; Koivisto *et al*., 2000), catecholamine producing M2 macrophages (Nguyen *et al.*, 2011), and direct sympathetic neuron innervation (Morrison *et al.*, 2008). When cold stimulated, locally produced and circulating catecholamines act as agonists to the α1 and β3 receptors to depolarize BAT cells, driving non-shivering thermogenesis (Koivisto *et* al., 2000). Simultaneously, blood flow increases to BAT and can account for up to ~40% of the total cardiac ejection fraction (measured in rats; Foster and Frydman, 1979). The blood is heated, returned to the heart by Suzler's vein, and redistributed to the organs (and not to peripheral sites such as the tail due to peripheral vasoconstriction) to maintain core temperature (Rauch and Hayward, 1969).

In addition to cold, non-shivering thermogenesis is inducible with high fat diets (Schulz and Tseng, 2013), cancer driven cachexia (Tsoli *et al.*, 2012), and pharmacologically with a β3 agonists such as norepinephrine (Foster and Frydman, 1979). Chronic pharmacological activation of BAT is actively being investigated as a treatment for metabolic syndrome, obesity, and diabetes (Shulz and Tseng, 2013).

BAT exhibits the capacity for moment-to-moment inducible thermogenesis via catecholamine agonists and increased blood flow and ability to expand thermogenic capacity over time via mitochondrial expansion and increasing UPC1 concentration. Cannon and Nedergaard summarize these phenomena as "BAT is both facultative and adaptive" (Cannon and Nedergaard, 2011).

When chronically cold-stressed, BAT mass, concentrations of mitochondria, UPC1 concentration, and thermogenic capacity increase (Lim *et al.*, 2012). With 2 to 8 weeks of conditioning, murine thermogenetic capacity increases to the point of being able to survive 4ºC (Lim *et al*., 2012). Additionally, non-shivering thermogenic capacity can be expanded from a second population of cells: white adipocytes. When stimulated by chronic cold, white fat adipocytes can take on brown fat-like phenotype known by several names: recruited BAT, beige fat, or Brite fat (Giralt and Villarrova, 2013). Beige fat expresses UCP1 and contains mitochronica, but at concentrations less than classic BAT (Giralt and Villarrova, 2013).

### d. **Core body temperature**

Unlike larger mammals, mice do not have stable core temperatures over time: core temperatures oscillate over short bursts of ~1ºC even within the TNZ (Gordon, 2009). In addition to short-term oscillation, there are circadian oscillations: mice in barren caging conditions maintain a core body temperature of 36.2ºC during the light cycle and 37.5ºC during the dark cycle as measured by intraperitoneal telemetry (Gordon, 2004). When provided deep bedding for nesting, core temperatures averages 37.2ºC and 37.5ºC during the light and dark cycles, respectively, as measured by intraperitoneal telemetry (Gordon, 2004).

The thermal biologist CJ Gordon (National Institute of Health) speculates mice conserve energy by allowing core temperature to fluctuate. Gordon considers mice facultative or “opportunistic” endotherms rather than true endotherms (Gordon, 2012).

## V. **Cold-stress and science**

Mice are routinely housed in sub-thermal neutral temperatures in barren cages that prevent behavioral thermoregulation (Gaskill *et al*. 2009). Subsequently, laboratory mice are cold-stressed. This cold-stress has major metabolic consequences (discussed in further detail in Chapter 2) and alters experimental results (discussed in detail in Chapter 3). Cold-stress is known to negatively impact models of oncology (David *et al.*, 2013b; Kokolus *et al.*, 2013), immunology (Romanovsky *et al.*, 1998; Rudaya *et al.,* 2005), obesity and metabolic syndrome (Lodhi and Semenkovich, 2009), neuroendocrinology (Baccan *et al*, 2010), and cardiovascular disease (Bartelt *et al.*, 2011; Swoap *et al*., 2008).

## VI. **Concluding thoughts**

Although cold-stress has been established to negatively impact numerous fields of science (Lodhi and Semendkovich, 2009; Karp, 2012), the solutions proposed thus far are piece-meal, applying to specific models, and are not reflected in the regulatory documents, e.g. the *Guide* (NRC, 2011), which allow mice to be housed at temperatures known to induce a wide range of cold-stress. We believe the true impact of cold-stress is not fully understood and likely has a substantial impact on most murine disease models. Additionally, most information on the thermoneutral zone of mice (and other rodents) has been gathered from individually housed animals using wire-screen or solid floors with no bedding, i.e. metabolic cages (Gordon, 2012). These cage environments ignore important elements of murine thermoregulatory biology such has huddling and nest building and do not represent the standard housing conditions (see chapter 2; Gaskill *et al*., 2012). Our knowledge of the thermoregulatory state of mice in routine housing is very limited (Gordon, 2012). All studies presented in this manuscript

are designed to measure the impact of cold-stress within modern vivariums and common housing systems.

Chapter 2: Characterizing non-shivering thermogenesis with thermography

This chapter is based on the following published works:

1. **David JM,** Chatziioannou A, Taschereau R, Wang H, Stout DB. 2013. The hidden cost of housing practice: using noninvasive imaging to quantify the metabolic demands of chronic cold stress of laboratory mice. Comp Med, 63(5): 386-91.
2. **David JM**, Stout DB. 2013. Poster: Quantifying Cold-stress in Laboratory Mice with Thermography: a non-invasive imaging technique. Am Assoc for Lab An Sci, Baltimore, MD.

## I. Introduction to Thermography

This chapter reports the initial observation of chronic non-shivering thermogenesis with thermography in mice housed in a modern vivarium and the subsequent validation work to establish thermography as a tool to measure cold-stress in mice. This chapter describes the correlation of non-shivering thermogenesis quantified with thermography to indirect calorimetry, a classic metric of cold-stress.

Thermal cameras detect infrared radiation emitted by an object. Using known physical properties of the object, thermography can be used to determine the temperature of the object (Speakman & Ward, 1998).

Like many other technologies, thermography cameras have recently increased in portability and resolution, while decreasing dramatically in cost (McCafferty, 2007). Previous thermography systems use liquid nitrogen to cool the detectors to reduce signal-to-noise ratios, limiting portability. Modern thermal cameras utilize electronic coolers that offer improved portability at reduced costs (McCafferty, 2007).

## II. Original observation

On passive observation with thermography, we noted mice housed in individually ventilated cages (IVC) exhibited a prominent heat signature from the interscpular BAT region compared to animals housed in static cages. Based on this observation, the following hypothesis was generated:

Mice housed in IVCs are more cold-stressed than mice housed in static cages.

Before the hypothesis could be tested, thermography based measurements of non-shivering thermogenesis needed to validated as a metric of cold-stress. To validate thermal imaging as a viable method, we compared thermography to indirect calorimetry, a well established method for determining energy use in mice.

## III. Indirect calorimetry and entropy production rate: a gold-standard of metabolic rate

Indirect calorimetry is the measurement of the free energy conversion to heat and application of thermodynamics to calculate metabolism. Indirect calorimetry is a classic measure of metabolism developed over a century ago (Atwater and Rosa, 1899). To calculate entropy production rate (EPR, calories expended per minute, cal/min), indirect calorimetry measures oxygen consumed ($VO_2$, mL/min) and carbon dioxide produced ($VCO_2$, mL/min) and apply the following stoichiometric formulas of biological combustion (Ferrannini, 1988):

$$1\text{ g Glucose} + 0.7\text{ L } O_2 \rightarrow 0.7\text{ L } CO_2 + 0.6\text{ g } H_2O$$

$$1\text{ g Lipid} + 2.0\text{ L } O_2 \rightarrow 1.4\text{ L } CO_2 + 1.1\text{ g } H_2O$$

From these stoichiometric formulas and the laws of thermodynamics, EPR (Ferrannini, 1988) can be calculated:

$$EPR\ (cal/min) = 3.91 * VO_2\ (mL/min) + 1.10\ VCO_2\ (mL/min)$$

### a. Substrate utilization

From the stoichiometric formulas of biological combustion, the use of either glucose or lipids as the primary energy substrate can be determined based on the

coefficient of $VO_2$ versus $VCO_2$ (see stoichiometric formulas above; Ferrannini, 1988). To determine to the substrate utilized, a unitless ratio called the respiratory quotient (RQ) can be calculated:

$$RQ = VCO_2 \div VO_2$$

RQ of 0.7 is indicative of oxidative lipolysis and RQ of 1.0 is indicative of oxidative glycolysis (Ferrannini, 1988). RQ values are between 1.0 and 0.7, indicating a mixture of lipids and carbohydrates are being utilized as energy substrates.

#### i. **Assumptions of indirect calorimetry**

Indirect calorimetry relies on several assumptions: biologic combustion of substrates is complete; the organism is neither acidotic or alkalotic, either of which can shift carbonic acid blood pools, changing the stoichiometric formula; and cellular respiratory chemical reactions apply to the entire organism (Ferrannini, 1988).

## IV. **Positron emission tomography**

Positron emission tomography (PET) imaging is a non-invasive imaging modality to measure metabolic aspects of *in vivo* tissues. Several excellent reviews and texts describing PET imaging have already been written (Phelps, 2006). PET will be briefly summarized here: a short lived positron emitting radioactive isotope is chemically bonded to a biologically active probe. The radio-probe is injected into a patient or pre-clinical animal. The probe circulates and mimics the biological pathways of the parent compound. The radio-isotope decays and produces gamma rays in the process. PET scanners detect the gamma rays and software reconstructs the raw data to produce a

3D image of where the probe accumulates. PET images can show a static snapshot of biodistribution at a given time or can show dynamic changes over time. PET is often supplemented by anatomical imaging, such as CT or MRI, to aid in localizing probe accumulation.

### a. $^{18}$F-Flurodoxyglucose

$^{18}$F-Flurodoxyglucose ($^{18}$F-FDG) is a biologically active analog of glucose. $^{18}$F-FDG is the most common PET probe and is utilized in the vast majority of clinical PET scans. Metabolically active cells take up the probe via glucose transporter in competition with endogenous glucose. $^{18}$F-FDG is phosphorylated within the cell by the enzyme hexokinase, trapping the probe in the cell, and causing measureable accumulation in glycolytic tissues (Phelps, 2006). $^{18}$F-FDG is used extensively to measure brain activity, heart tissue viability, in oncology, and numerous other applications. In this work, we use $^{18}$F-FDG PET to measure glucose kinetics of BAT.

## V. Validation of thermography as a metric of cold-stress

To validate thermography based quantification of non-shivering thermogenesis as a surrogate metric of cold-stress, we measured non-shivering thermogenesis with thermography against better established measurements of metabolism: indirect calorimetry and positron emission tomography.

### a. **Thermography correlation with entropy production rate**

#### i. **Method**

Specific pathogen free, 10 to 12 week old mice (hirsute C57Bl/6j and nude Crl:Nu-*Foxn1*$^{nu}$ ♂ and ♀, n = 5 per strain/stock per gender) housed in IVC on corncob bedding at 20-21°C (Innovive, San Diego, CA) were acclimated for 1 hour at 21°C, 26°C, and 31°C in a cross-over study design between the hours of 09:00-10:00 to control for circadian rhythm (van der Veen *et al.*, 2012). 21°C represents "room temperature" commonly found in mouse vivariums and imaging centers. 26°C is the upper boundary of regulatory allowed housing conditions (NRC, 2011). 31°C approximates thermoneutrality of hirsute mice (Gordon, 2012). After 1 hour of acclimation, the mice were sealed in an air-tight cage and baseline $VO_2$ and $VCO_2$ were measured (models 17624 and 17630, respectively, Vacumed, Ventura, CA; equipment and consultation provided by Dr. Kenneth Roos). Before each sampling period, the gas monitors were calibrated using a reference gas per the manufacturer's instructions (Vacumed, Ventura, CA). After 1 hour in the sealed cage, $VO_2$ and $VCO_2$ were resampled to calculate EPR and RQ. Each $VO_2$ and $VCO_2$ sample required 30 seconds. Non-shivering thermogenesis was calculated as ΔT BAT by measuring the emitted heat from the BAT region and subtracting an internal control region (Figure 2-1). Emissivity, a unitless ratio of measured emitted temperature against a hypothetical pure emitter, of fur was set post-data collection to 0.94 and the skin of nude animals to 0.98 (Gieger, 2009).

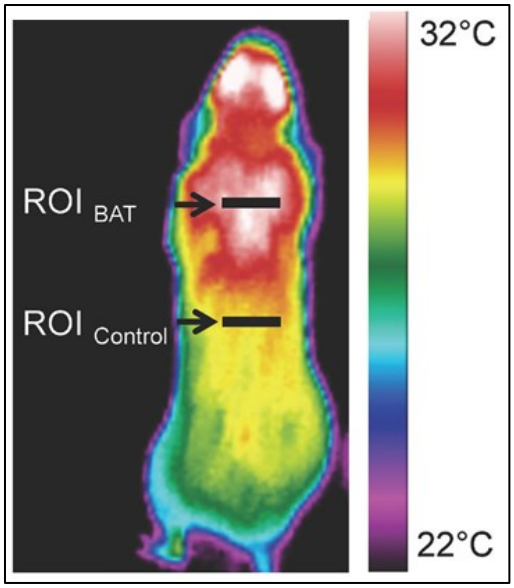


**Figure 2-1** Thermography regions of interest for determining non-shivering thermogenesis is quantified by drawing a line profile indicating a region of interest (ROI) across the interscapular brown adipose tissue region and subtracting an internal control region at the most caudal rib (black arrows; C57BL/6J mouse).

The effects of interactions between environmental temperature, sex, and strain (i.e. inbred) or stock (i.e. outbred) on EPR, RQ, and ΔT BAT were tested using a nonlinear mixed-model effects model (R Studio; Pinheiro and Bates, 2000) with the following formula where $Y_0$ is the intercept of ΔT BAT on the y-axis:

Y = mouse (sex, strain/stock) + sex + strain/stock + temperature + (sex * strain/stock) + (sex * temperature) + (strain/stock * temperature) + (sex * strain/stock * temperature)

Significance was determined by post-hoc test with a Tukey correction for multiple comparisons. *P* value less than 0.050 was considered to be significant. The model assumptions of normality and homogeneity were tested post-hoc. The correlation of ΔT BAT and EPR was calculated with the coefficient of determination ($R^2$) and the formulaic relationship was determined using regression modeling (R studio).

### ii. **Results**

For all groups, EPR increased ($P < 0.001$) with progressively lower temperatures (Figure 2-2). For all groups except C57BL/6J female mice, RQ significantly ($P < 0.001$) increased as environmental temperature decreased (Figure 2-2); RQ in C57BL/6J female mice significantly ($P < 0.01$) increased as temperatures decreased from 31°C to 21°C (Figure 2-3). According to both ΔT BAT and EPR, female and male mice Crl:Nu-*Foxn1*$^{nu}$ experience significantly ($P < 0.001$) greater metabolic stress than their C57BL/6J counterparts at all tested temperatures. Non-shivering thermogenesis as measured by ΔT BAT did not vary significantly by sex among C57BL/6J or Crl:Nu-*Foxn1*$^{nu}$ mice. Sex did not alter EPR in C57BL/6J mice, but male Crl:Nu-*Foxn1*$^{nu}$ mice exhibited significantly ($P < 0.001$) greater energy expenditure at 21°C and 26 °C—but not at 31 °C—than did their female counterparts.

From 31 to 21 °C, EPR increased significantly ($P < 0.001$) more in male Crl:Nu-*Foxn1*$^{nu}$ mice (175%; SE 5.51) than in male C57BL/6J mice (98% SE 7.62) and in female Crl:Nu-Foxn1nu mice (115%; SE, 6.04) than in female C57BL/6J mice (89% SE 7.3; Figure 2-2). Similarly, RQ increased significantly ($P < 0.001$) more in Crl:Nu-*Foxn1*$^{nu}$ mice (female: 17%; SE, 3.14; male: 26%; SE, 3.28) than in C57BL/6J mice (female: 10%, SE, 3.19; male: 20%, SE, 3.40) from 31°C to 21°C.

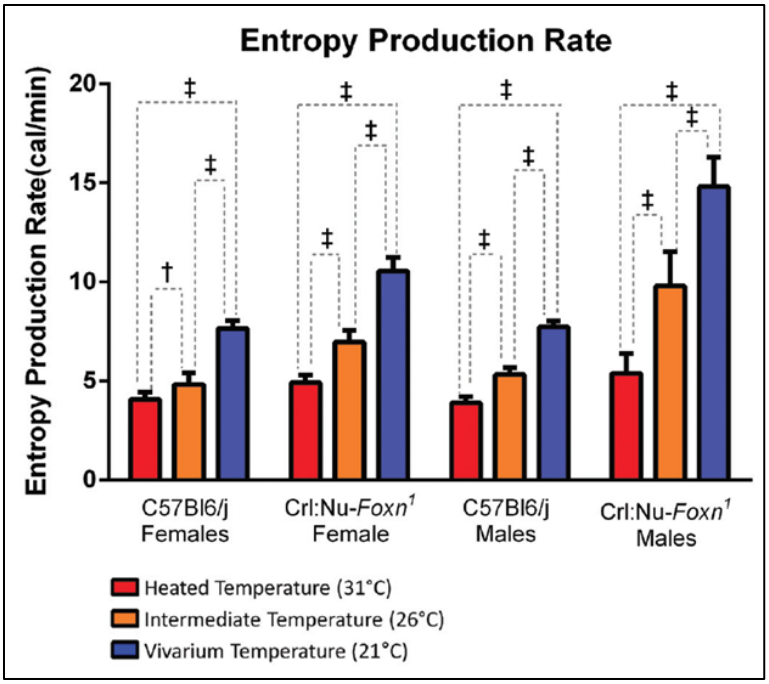


**Figure 2-2**. Influence of ambient temperature on entropy production rate (n = 5 per gender per phenotype). Bars represent standard error. †, $P < 0.010$; ‡, $P < 0.001$

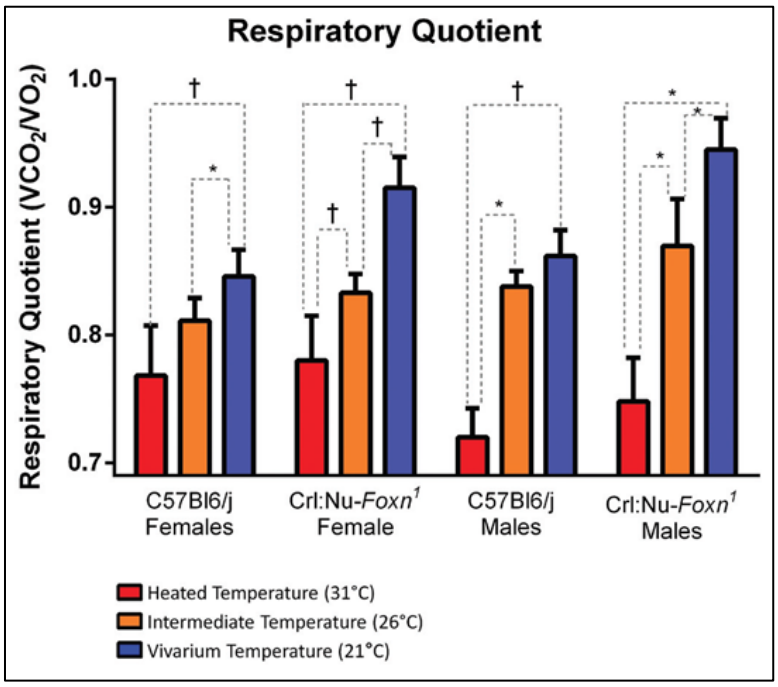


**Figure 2-3** Influence of ambient temperature on respiratory quotient (n = 5 per gender per phenotype). Bars represent standard error. †, $P < 0.010$; ‡, $P < 0.001$

In all groups, ΔT BAT increased significantly ($P < 0.001$) as environmental temperature decreased (Figure 2-4). Regardless of sex, Crl:NU-*Foxn1*$^{nu}$ mice exhibited significantly ($P < 0.001$) greater non-shivering thermogenesis than did C57BL/6J mice (Figure 2-4 and 2-5).

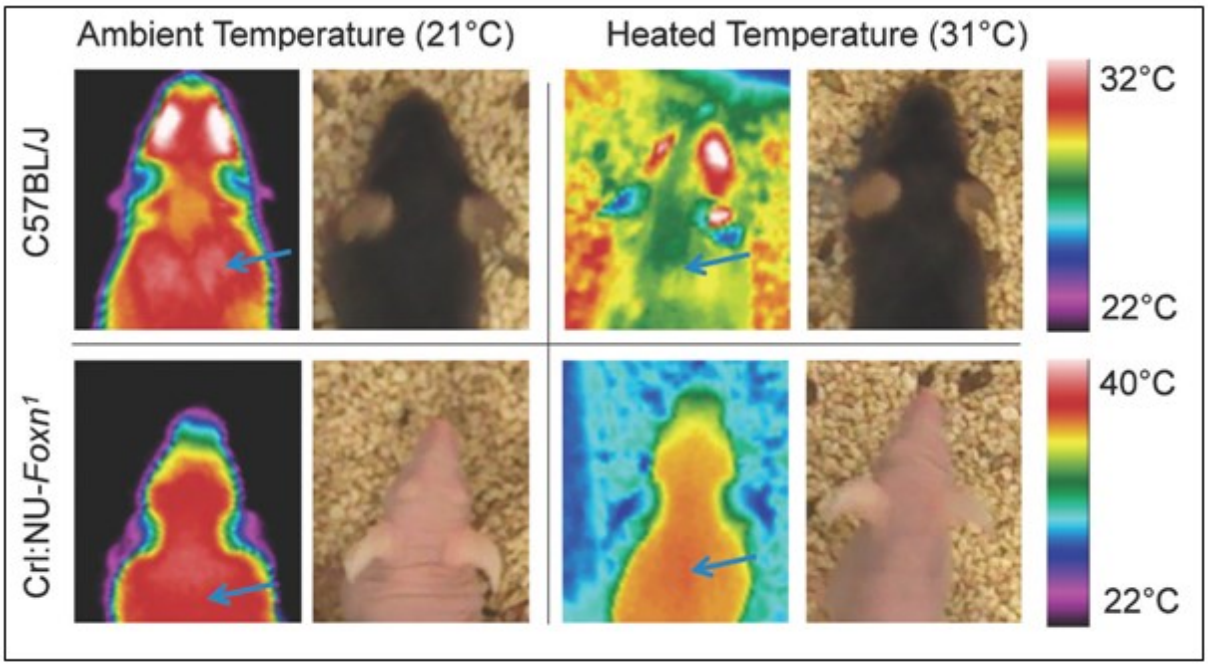


**Figure 2-4**. Effect of vivarium temperature on non-shivering thermogensis (blue arrow) visualized by thermography.

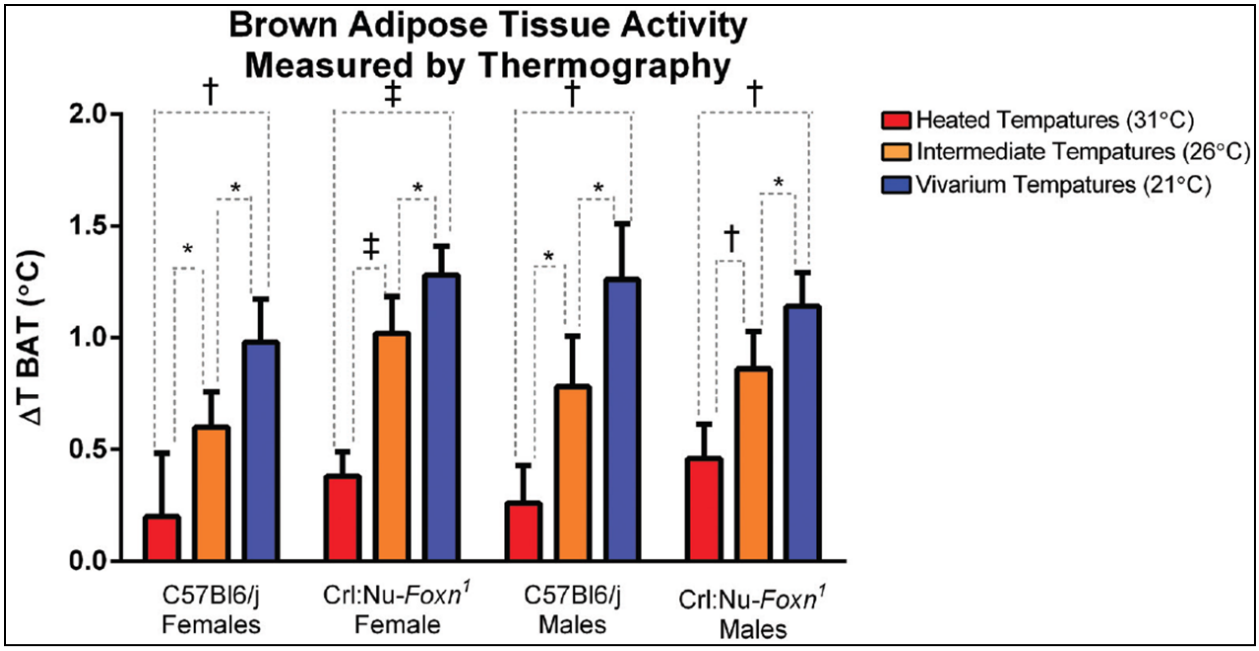


**Figure 2-5**. Quantifcation of non-shivering thermogenesis measured with thermography (n = per gender per phenotype). Errors represent standard error. *, $P < 0.050$; †, $P < 0.010$; ‡, $P < 0.001$

ΔT BAT and EPR significantly correlated in all groups ($P < 0.001$; Figure 2-6).

The formulaic relationship between ΔT BAT and EPR is defined below (Table 2-1).

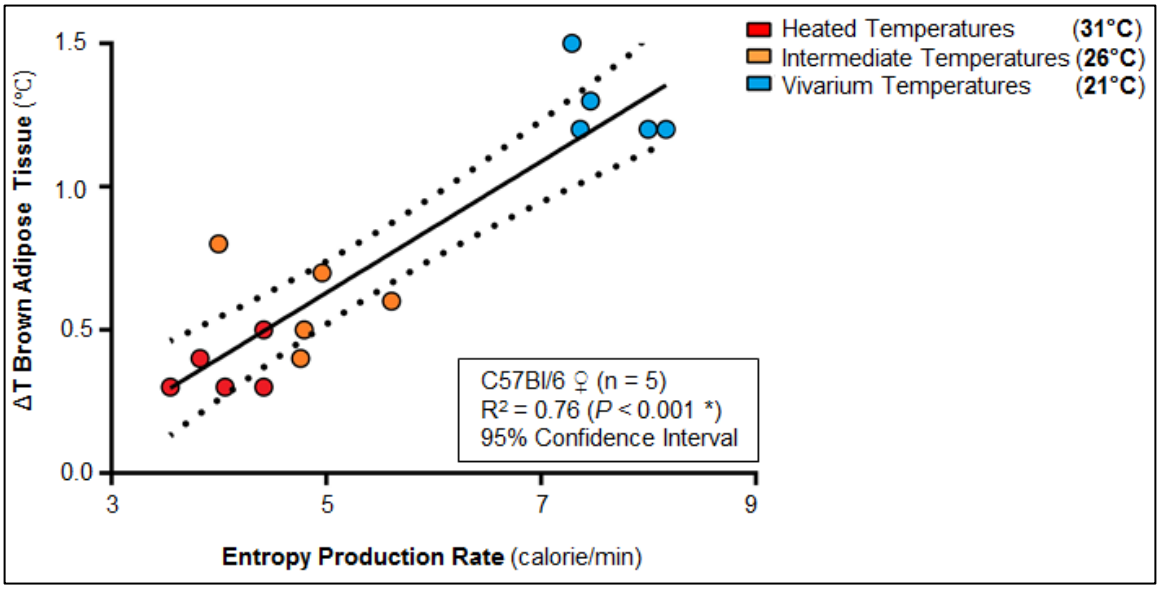


**Figure 2-6** Correlation of non-shivering thermogenesis and entropy production rate (n = 5 female C57BL/6 mice).

| Formulaic Relationship Between ΔT BAT and EPR | | | |
|---|---|---|---|
| Nu-*Foxn1*$^{nu}$ ♀ | EPR (calories/min) = | 3.781 × ΔT BAT (°C) + | 4.228 |
| Nu-*Foxn1*$^{nu}$ ♂ | EPR (calories/min) = | 3.781 × ΔT BAT (°C) + | 3.969 |
| C57BL/6 ♀ | EPR (calories/min) = | 3.781 × ΔT BAT (°C) + | 3.138 |
| C57BL/6 ♂ | EPR (calories/min) = | 3.781 × ΔT BAT (°C) + | 2.879 |

Slope Intercept

| Group | $R^2$ |
|---|---|
| Nu-*Foxn1*$^{nu}$ ♀ | 0.69 ($P < 0.001$ *) |
| Nu-*Foxn1*$^{nu}$ ♂ | 0.62 ($P < 0.001$ *) |
| C57BL/6 ♀ | 0.76 ($P < 0.001$ *) |
| C57BL/6 ♂ | 0.69 ($P < 0.001$ *) |

**Table 2-1.** Formulaic relationship between ΔT BAT and EPR (n = 5 per gender per phenotype). *, $P < 0.001$

### b. Thermography correlation with $^{18}$F-FDG uptake experiments

Based on the glycolytic switch observed on the RQ (Figure 2-3), we hypothesized the metabolic switch towards glycolysis observed by indirect calorimetry was being driven by BAT metabolism. To test the hypothesis, positron emission tomography (PET) was used to evaluate the glucose analog $^{18}$F-FDG to measure glycolytic activity of BAT.

#### i. Method

To quantify the relationship of thermography based assay of non-shivering thermogenesis and BAT glucose uptake, mice were acclimated (C57Bl/6j ♀, n = 5, cross-over study design) to 21°C and 31°C for 1 hour. The acclimation time was selected because in pilot studies indirect calorimetry values stabilized after ~40 minutes. Conscious mice were injected with ~35 μCi of $^{18}$F-FDG, allowed 50 minutes of uptake

period, anesthetized with ~2% isoflurane mixed in 100% $O_2$, and a PET image acquired for 10 min followed by a single projection X-ray (Genisys4, Sofie Biosciences, Culver City CA). The PET images were generated by using a maximum likelihood expectation maximization algorithm (Lange and Carson, 1984) for reconstruction using 60 iterations, normalized for detector response and corrected for isotope decay and photon attenuation (algorithm was developed by Richard Taschereau, University of California, Los Angeles). Using the Mouse Atlas Registration System (Wang *et al.*, 2012a; Wang *et al.*, 2012b), the single projection X-ray radiograph was used to generate an atlas of mouse organ locations and a coregistered standardized $ROI_{BAT}$ for the location of the BAT. PET images of BAT $^{18}$F-FDG uptake were analyzed (AMIDE v1.0.1.; http://freecode.com/projects/amide/releases/339498) to calculate total activity. Total $^{18}$F-FDG uptake in the $ROI_{BAT}$ (as defined as by the Mouse Atlas Registration System) was divided by the total injected dose (determined as a whole-body ROI) and expressed as a percentage of the injected dose. Significance of $^{18}$F-FDG BAT uptake was calculated by one-way ANOVA with a post-hoc test with a Holms-Sidak correction for multiple comparisons and an α cut off of 0.050 for significance.

The correlation between BAT $^{18}$F-FDG and ΔT BAT was determined via a coefficient of determination calculation ($R^2$; R, R Studio, Boston, MA).

### ii. **Results**

$ROI_{BAT}$ uptake of the injected dose of the glucose analog $^{18}$F-FDG increased significantly ($P < 0.001$) from 1.10% ID, SE 0.09 at 31 °C to 4.33% ID, SE 0.86 at 21ºC

(Figure 2-7). BAT ID% and ΔT BAT correlated significantly ($R^2$ = 0.71, $P$ < 0.001; Figure 2-8).

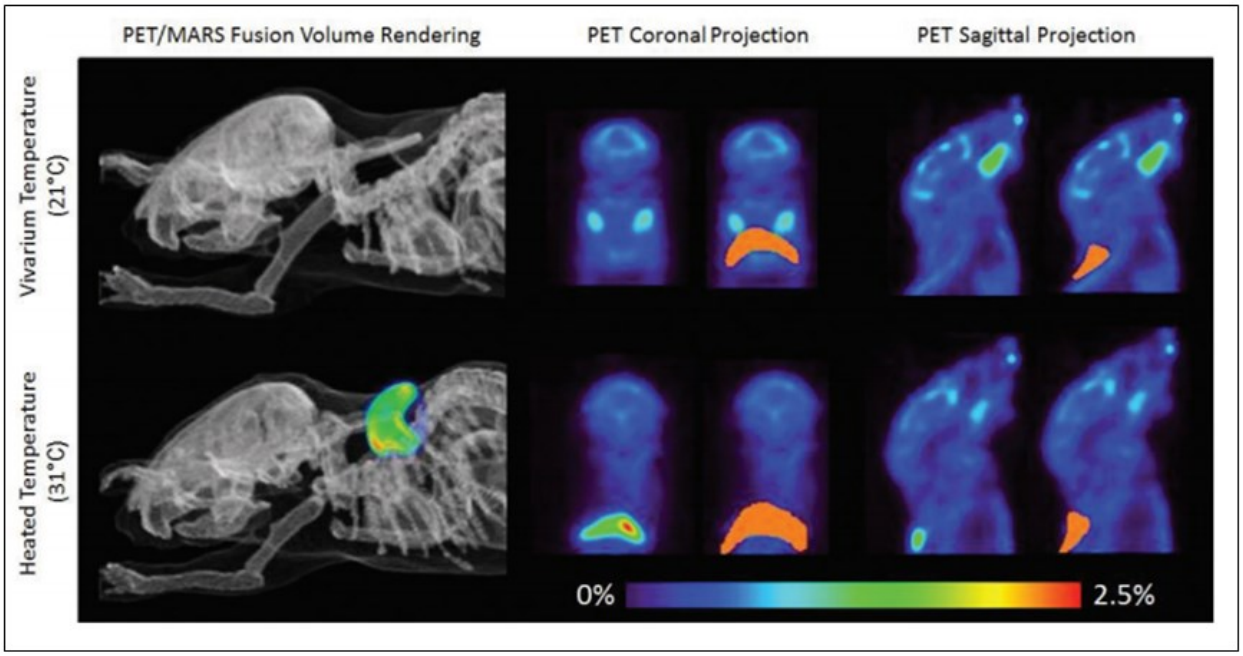


**Figure 2-7** Influence of ambient temperatures on brown adipose tissue glucose uptake as measured by positron emission tomography. Computed tomography and positron emission tomography scan with the glucose analog probe $^{18}$F-fluorodeoxyglucose where uptake occurs at an ambient temperature of 21°C or 31°C (n = 4 C57BL/6 females, cross-over study). The images on the left panel are volume rending of the atlas. The right panels are 0.2-mm slice coronal and sagittal PET projections across the BAT region. Standardized BAT regions (orange, generated by using the Mouse Atlas Registration system). The scale bar is percentage injected dose.

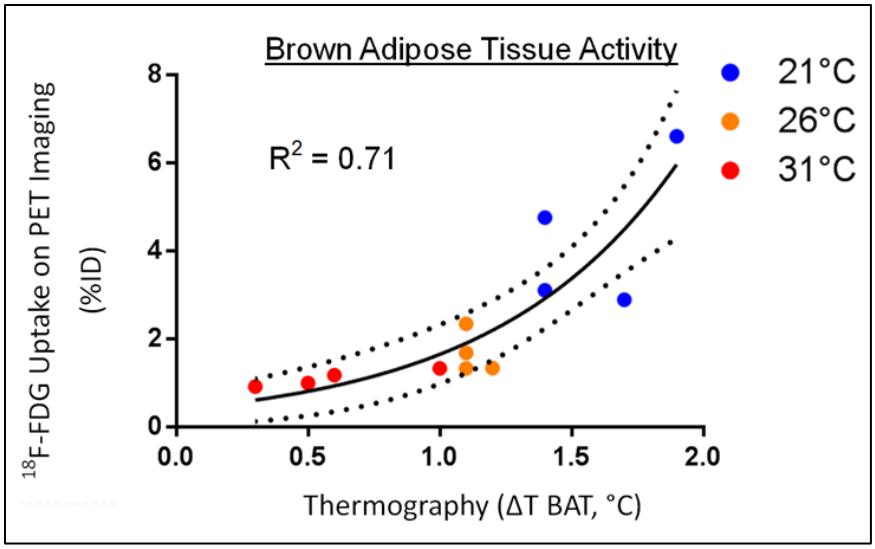


**Figure 2-8** Correlation of non-shivering thermogenesis and brown adipose tissue $^{18}$-F-FDG uptake in BAT (n = 4 C57BL/6 female mice)

## VI. Discussion

We demonstrated that mice are physiologically stressed under routine vivarium temperatures despite being housed within the regulations set by the *Guide* (NRC, 2011). Through indirect calorimetry and RQ calculations (Ferrannini, 1988), we show that mice respond to this temperature by fundamentally shifting their global glucose utilization. By using noninvasive *in vivo* $^{18}$F-FDG PET imaging, we demonstrate that the metabolic shift towards glucose metabolism is being driven (at least in part) by BAT. The increased EPR under routine vivarium temperatures mirrors the temperature-dependent metabolic rate increase seen in steel-box calorimeter-based experiments (Gordon, 1985). Using another noninvasive imaging technology, infrared thermography, we demonstrate that non-shivering thermogenesis occurs concurrently with high glucose BAT uptake. Through these 3 noninvasive, independent metrics of metabolism, we demonstrate that routine vivarium temperatures drive high glucose metabolism to fuel non-shivering thermogenesis, which accounted for nearly half of the energy

expenditures of hirsute mice housed at 21°C. Even at the upper end of the Guide recommendation of 26ºC, there is still a significant cold stress effect. This suggests that simply raising the temperature to the upper end of the recommended range is insufficient to eliminate cold stress impact on mouse models.

We also demonstrate through calculations of EPR, RQ, and ΔT BAT that nude mice were significantly more metabolically stressed than hirsute mice at all tested temperatures. For nude mice, energy expenditure at 21 °C was more than twice that at heated temperatures. Although it should be no surprise that nude mice experience greater cold stress in light of previous observations that they have high feed consumption relative to body mass (Weigh, 1984) and lack of insulation (Cannon and Nedergaard, 2011), “there is surprisingly little information on their thermoregulatory characteristics” (Gordon, 2012). These results exemplify a key and commonly underappreciated aspect of research using mice: different strains, transgenic mice with altered metabolism, and mice with different phenotypes can experience different amounts of physiologic stress relevant to the ambient temperature. These findings have board implications on murine dependant research.

## VII. **Considerations when using thermography to measure non-shivering thermogenesis**

Thermography is a powerful, inexpensive tool to measure cold-stress in mice that is portable, allowing measurements in the vivarium. Thermography data acquisition does not require anesthesia unlike other imaging modalities such as PET. Anesthesia alters physiology (Fueger *et al*., 2006), limiting serial sampling, and the stress of handling

during the anesthesia can mask cold-stress (Rosmasosky *et al.*, 1998). Thermography lacks these disadvantages and has much shorter sampling frequency.

The thermography methods presented above are sensitive to technique. Important details for the successful measure of non-shivering thermogenesis with thermography are described below.

a. **Thermography factors**

i. **Emissivity**

"Emissivity" is the property of a body to emit infrared waves in proportion to its temperature. In thermography, emissivity can be set in post-data handling to a unitless ratio of infrared emission rates to a hypothetical pure emitter (dubbed a "black body"). The emissivity of fur is ~0.94, while nude skin is ~0.98 (Gieger, 2009). If emissivity is of an object is unknown, it can be roughly estimated by adhering black electrical tape to the object, allowed the temperature to equilibrate, and the taking the ratio between the emitted temperature of the object divided by measured temperature the black tape.

ii. **Resolution**

Poor resolution leads to blurring and difficultly in analyzing thermal images. Such low resolution leads to a blurring of anatomical structures, greatly complicating ROI placement (Figure 2-9). Consequently, using a low resolution thermography camera leads to less reproducible results.

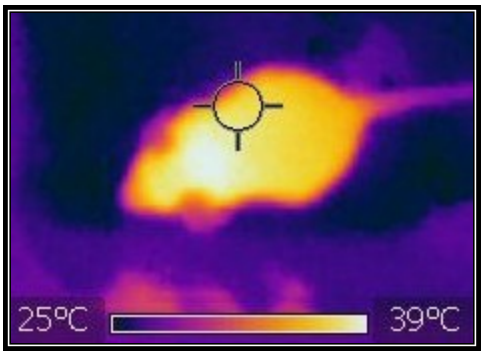


**Figure 2-9** Low resolution (FLIR i5, 60x60 pixel) thermal image illustrating loss of anatomical information in a C57BL/6J mouse.

iii. **Tripod**

Use of a tripod allows the operator to use one hand to take images and another to manipulate the animals. The tripod also allows a consistent distance to the mouse, thus maintaining the size of the mice in the images and enables consistent ROI sizes for image analysis. The stable mount for the camera together eliminates motion blurring caused by holding the camera and pushing on buttons by hand. When considering purchase of a thermography camera, we recommend a camera with a standard 3/4" mount for tripod mounting. A remote trigger may also be useful.

b. **Mouse factors**

i. **Mouse body posture**

Head position is key: if the head is elevated, small skin folds occur at the base of the neck, creating thermal streaking across the BAT region, complicating ROI placement. If the head is pointed down (towards the floor) or the animal is hunched, the fur parts revealing the underlying skin, which will be significantly warmer than the fur-insulated control region. Hunched posture greatly complicates data analysis of thermal images (Figure 2-10).

There are 2 approaches to ensuring a level head position: take 3 images of each mouse per time point and select the first image with a head position parallel to the ground; or applied gentle traction on the tail. The mouse will push against the traction, leaning the head forward and parallel to the ground. In our experience, either technique will yield consistent results. Applying traction to the tail is faster and best when there are large number of mice in the cage (e.g. 5) to minimize the time between opening the cage and disturbing the animals and data acquisition. For consistency, we applied traction to the tail for all image acquisitions.

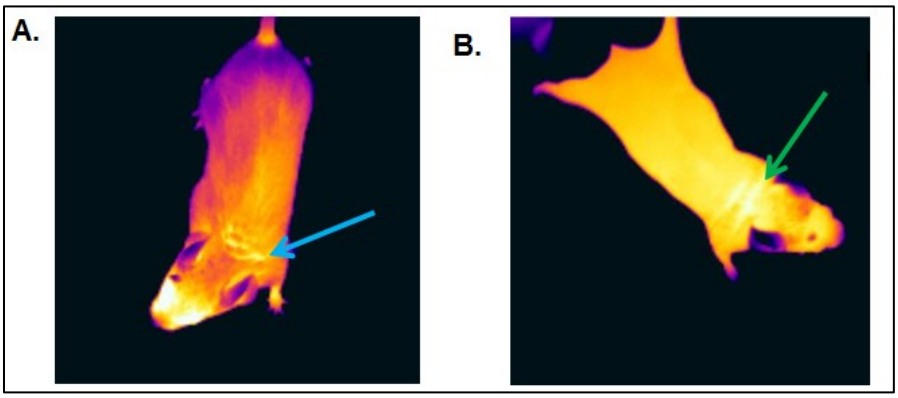


**Figure 2-10** Effect of mouse posture on thermography measurements of non-shivering thermogenesis. (A) Head posture can part the fur (blue arrow) revealing the underlying skin (*Prkdc*$^{scid}$) or (B) cause skin folds (green arrow; Nu-*Foxn1*$^{nu}$) to form over BAT region, complicating region of interest placement.

ii. **Fur**

Fur is an insulator, providing a barrier between the body heat signal and the thermal camera. Heat radiates through the fur via four mechanisms: convection between the fibers, radiation, evaporation of water, and, most importantly, conduction through the fibers (Hammel, 1955). Because of the insulative effect, fur coats (or lack thereof in nude mice) must be uniform for thermal quantification (Purohit and McCoy,

1980). Patchy fur loss in the regions of interest due to age or barbing reveals the underlying skin and complicates quantitation of non-shivering thermogenesis with thermography.

### iii. **Circadian rhythm**

Sampling time of day can dramatically alter cold-stress experienced by mice. Mice are most cold-prone during the light, when physical activity is minimal (Figure 2-11; Gordon, 2012). Mice are relatively cold-resistant during the dark cycle, when mice are physically active (Figure 2-11; Gordon, 2012).

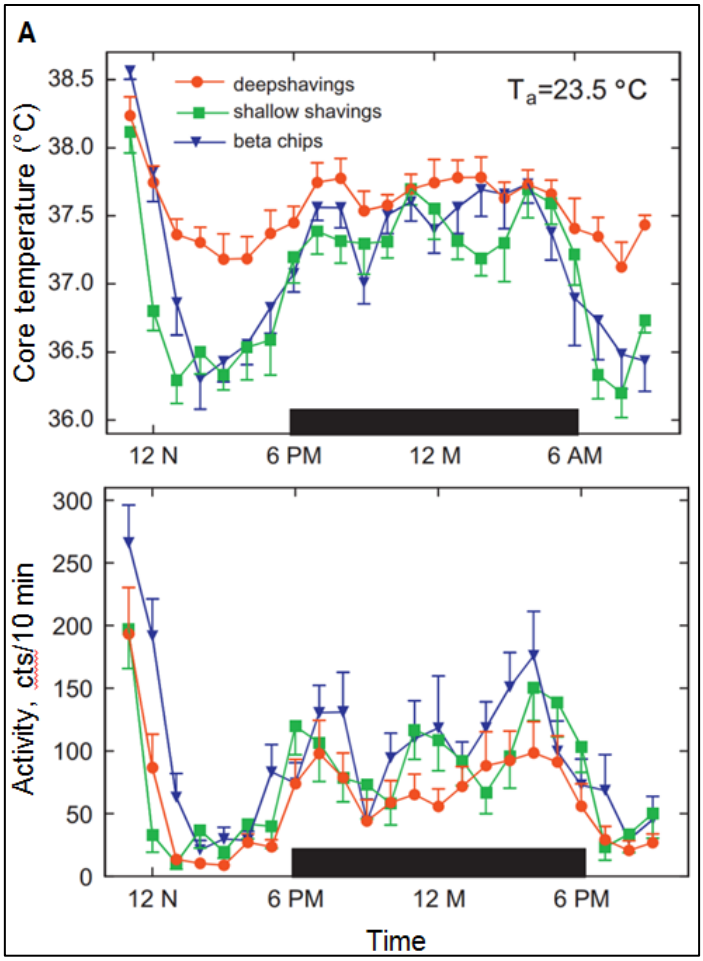


**Figure 2-11** Influence of circadian rhythm on thermoregulatory needs and physical activity. "Time course of core temperature of group housed, female CD-1 mice (4 per group) at 22°C in cages with either ample pine shaving bedding for burrowing (deep shavings) or minimal amounts of bedding material (shallow shavings or beta chips) of inadequate depth where mice could not borrow." Reprinted from Gordon (2012) with permission.

iv. **Animal age**

Older animals have a reduced capacity for non-shivering thermogenesis (McDonald *et al.*, 1989). Unless there is an experimental rationale to the contrary, animals should be aged matched when comparing cold-stress between groups of animals.

c. **Data collection**

### i. **Skill**

Proper technique is key to developing speedy acquisition times to minimize handling induced hyperthermia (Rosmasosky *et al.*, 1998) and transiently reducing cold-stress. We recommend extensive practice prior undertaking any experiment so that measurements can competently be acquired quickly. According to our experience, when adequate skill is developed, variation between rapid, multiple-sampling of the same animal should vary $\leq$ 0.2 °C.

### ii. **Sampling time**

Related to skill, sampling time is of the utmost importance: BAT activity can change very quickly. Excessive time handling mice will result in stress induced hyperthermia (Rosmasosky *et al.*, 1998), potentially confounding thermography based quantification of non-shivering thermogenesis. The animals cannot be removed from the vivarium for accurate measurements due to handling induced hyperthermia (Rosmasosky *et al.*, 1998). Therefore, sampling within the animal room is required. Mounting the thermal camera on a tripod in the biosafety cabinet and pre-marking the mice with easily identifiable marks greatly facilitates rapid data acquisition. After considerable practice, our sampling time of approximates 15 seconds per cage plus 7 seconds per mouse in each cage. If the cages are left undistributed until the data acquisition, the time between cage sampling is likely not important.

## a. **Data processing**

### iii. **Regions of interest**

Selecting and drawing regions of interest (ROI) in a consistent and uniform manner is essential. A good ROI has the following characteristics:

-Similar fur thickness (Purohit and McCoy, 1980)

-Anatomic landmarks that facilitate consistent ROI placement

-When adequately described, is reproducible independent of personnel analyzing data

The mouse's body is roughly cylindrical in shape and the signal decreases towards the lateral aspects of the animal (Figure 2-1). Drawing the line profile over the dorsal midline minimizes include the diminishing signal on the edges.

## VIII. Recommended specifications of thermal cameras to measure non-shivering thermogenesis

There is a large spectrum of available thermography cameras, ranging from very inexpensive, low resolution to very expensive, high resolution. Based on our experience, the following specifications of thermography cameras are recommended to utilize the techniques described in this chapter:

- Minimal focal distance of $\leq$0.6 meters for working within biological safety cabinets
- Standard ¾" camera mount for tripod utilization
- Resolution of at least 320 x 240 pixels
- Given the small spectrum of $\Delta$T BAT, a sensitivity of $\leq$ 0.1°C
- Manual focus

- Portable form factor to facilitate data collection in the vivarium to minimize alterations in BAT activity
- Certified calibration

## IX. Concluding remarks on thermography

When the operator is properly trained, thermography is a powerful, economical, high-throughput tool to measure non-shivering thermogenesis. It should be recognized that sampling is a single instance and does not represent an entire 24 hour period. Non-shivering thermogenesis is subject to large, circadian driven swings in activity (Sutton *et al*., 2012). Circadian rhythm should always be considered in experimental designs utilizing thermography to measure non-shivering thermogenesis.

In addition to husbandry applications, the techniques described here might be applicable to BAT, metabolic, diabetes, and obesity studies.

Chapter 3: Experimental implications of housing dependent cold stress variations

This chapter is based on the following published works:

1. **David JM**, Knowles S, Lamkin D, Stout DB. 2013. Individually Ventilated Cage Impose Cold-stress on Laboratory Mice: a source of experimental variability. J Am Assoc Lab Anim Sci, 52(6): 738-44.
2. **David JM**, Stout DB. 2013. Presentation: Individually Ventilated Cages, an Experimental Confounder. AALAS, Baltimore, MD.

## I. History of individually ventilated cages

Laboratory mouse caging has undergone dramatic changes over the past century: originally cages were simple “shoe boxes” made of cheap materials such as wood or steel with wire bottoms to allow waste material to fall out of the cage. It is well established via preference testing that rodents have a strong preference for solid bottom caging with bedding (“contact bedding”) over wire frame cage bottoms (Stark, 2001; Milite, 2008). Caging standards changed to solid bottom due to welfare concerns (NRC, 2011).

Overtime, the scientific community became aware of murine pathogens and the effect on research results, such as tumor formation rates, decreased breeding efficacy, and reduced experimental reproducibility (Nikclas *et al.*, 1999). As demands for specific pathogen free animals increased, novel engineering controls were developed. The two most important pathogen engineering controls are microisolator cages and Illinois cabinets. Microisolator cages have a lid fitted with a filter (Figure 3-1). These microisolator cages provided excellent pathogen control, but reduced free gas exchange (Hasenau *et al.*, 1993; Mamarzadeh, 1998). *In silico* simulations estimate the cage air changes per hour (ACH) in open top cages approximately matches room air exchange rates (typically, 10-15 ACH; NRC, 2011). Microisolator lids reduce air exchange by ~2 orders of magnitude (0.15 – 0.18 ACH; Mamarzadeh, 1998), causing a high accumulation of gaseous waste. In microisolator cages with 5 CD-1 female mice, $CO_2$ concentrations average 5600 parts per million (ppm) by day 5 post cage change and ammonia reaches an average of 47.8 ppm by day 8 post cage change (Memarzadeh *et al.*, 2004). Concentrations of $NH_3$ over 52 ppm are associated with

respiratory and ocular lesions (Vogelweid *et al*, 2011) and are a major determinant of cage change intervals.

Illinois cabinets are self-contained units that house mouse cages (Figure 3-1). Illinois cabinets have a high degree of environmental and pathogen control, but are expensive and have limited holding capacity. The low holding capacity, bulk, and cost of Illinois cabinets limit their use to special cases, e.g. immunocompromised animals (Milite, 2008). Illinois cabinets can still be found in ~30% of animal facilities (Doughman, 2013).

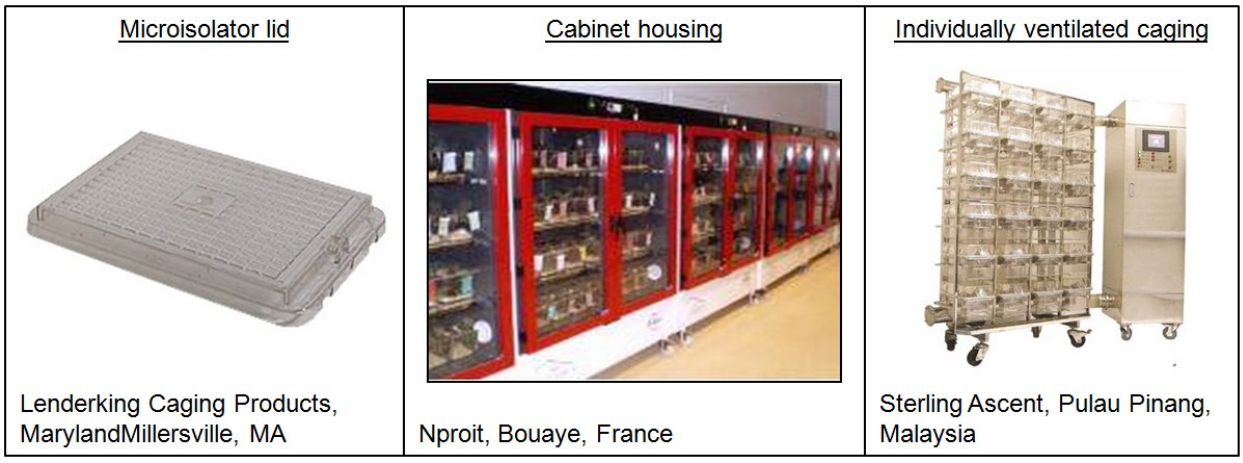


**Figure 3-1** Mouse caging examples.

Attempts to control the increased waste gases and moisture in flattop micro-isolator cages inspired the next generation of mouse housing systems. The current state of the art cage design is the individually ventilated cage (IVC; Doughman, 2013).

Thoren introduced the first commercial IVC in 1979. Many different iterations are available today. IVCs are designed to minimize waste gas, facilitate high stocking densities, to make efficient use of vivarium floor space (Milite, 2008). IVCs have nearly

doubled the number of mice per square foot of vivarium compared to microisolator cages and ~four times compared to Illinois cabinets.

IVCs mechanically supply air into and/or exhaust air out of the cage. The IVC can over-supply air, to create a positive pressure compared to the room ("barrier") to exclude pathogens from the cage. Alternately, IVCs can under supply air by increased exhaust pressure to create negative pressure relative to the room ("containment") to contain pathogens within the cage. To effectively evacuate waste gases, the air within the cage is turned over 60 to 80 times per hour (Milite, 2008). Most IVC maintain airflow supplied at 0.2 m/s. Air flows above 0.2 m/s are associated with weight loss and reduced weaning survival rates (Lipman, 1999).

IVC are the current *de facto* state of the art caging system for laboratory mice: they can be found in ~70% of all US vivariums and are the fastest growing segment of mouse caging (Doughman, 2013) due to high stocking density per square footage of vivarium space, reduced waste gas accumulation (Hoglund and Renstrom, 2000), excellent murine and experimental pathogen control (Brielemier *et al.*, 2006; Compton *et al.*, 2004), lower allergen exposure to staff (Reeb-Whitaker *et al.*, 1999), and prolonged cage change interval (from 1 week to 2 weeks).

a. **Airflow**

IVC improve murine care and lower animal care labor costs. Through preference testing, air flow is known to be aversive to mice (Baumans, 2002). Even small air speeds reduce the thermal resistance of mice (Chappell and Holsclaw, 1984). Air speeds of 0.25 m/s (similar to speeds found in most IVC) at 20ºC are known increase

oxygen consumption by ~30% in deer mice (Figure 3-2; Chappell and Holsclaw, 1984). Increasing wind speeds shift the animal's thermoneutral temperature range upwards (Chappell and Holsclaw, 1984).

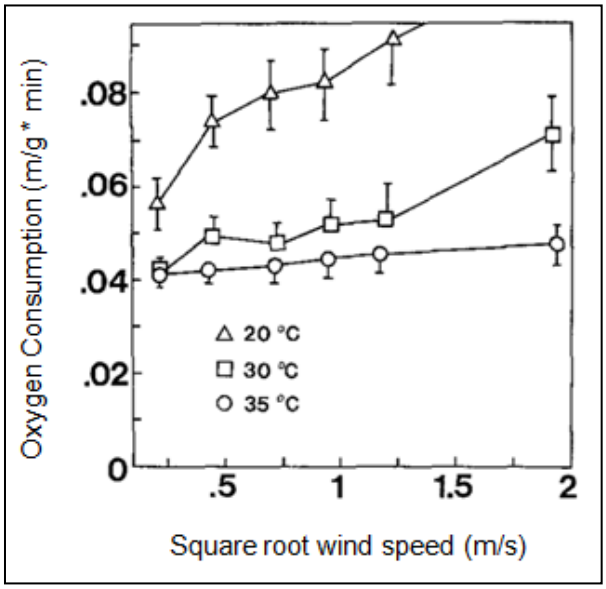


**Figure 3-2** "Oxygen consumption as a function of wind speed at three ambient temperatures" in deer mice. "Vertical lines are two standards errors." Reprinted from Chappell and Holsclaw (1984) with permission.

## II. Individually ventilated cages induce cold-stress

Based on the original thermography observations of systemic, chronic non-shivering thermogenesis previously described (chapter 2) and the air flow within IVC, we developed three hypotheses:

(1) the mice housed within IVC are cold-stressed compared to static cages;

(2) the additional cold stress imposed by IVC affects the results of experiments using mice to model human disease; and

(3) the additional cold stress can be mitigated by the addition of shelters in the environment.

In this work we measure the effect of IVC housing on subcutaneous xenograph tumors. We selected subcutaneous xenographs as our model of interest because it is common, central to oncology research, and peripheral most likely to be vulnerable to cold due to their peripheral location.

### a. **Methods**

Specific pathogen free CB17/Icr-*Prkdc*$^{SCID}$ and Crl:Nu-*Fox1*$^{nu}$ 10 week old male mice were housed in an Association for the Assessment and Accreditation of Laboratory Animal Care, international accredited facility, fed a routine commercial diet (NIH31, Harlan Teklad, Madison, WI), and received HCl acidified water (pH 2.5) reverse-osmosis-purified water *ad libitum*. The room was maintained at 21°C with a relative humidity of 30% to 70% and 10 to 15 air changes per hour. After a 72 hour acclimation period, the mice were evenly divided into single housing in static cages (Innovive, San Diego, CA), IVC with 60 ACH at 0.2 m/s "U" shaped air flow (Innovive, San Diego, CA), or IVC with shelters (InnoDome, InnoVive, San Diego, CA). Each cage contained 200 g of corncob bedding. Each cage was changed every 7 days to maintain consistency between groups.

To assay cold-stress, non-shivering thermogenesis was measured with thermography (see Chapter 1) for 7 days between the hours of 0900 and 1000 to control for circadian rhythm (van der Veen *et al.*, 2012). After a 7 day baseline, human epidermoid carcinoma cells (A431, $10^6$ cells) suspended in 50% PBS/50% Matrigel (Fisher Scientific, Pittburgh, PA) were subcutaneously injected. The cells were grown under routine conditions: sterile, DMEM supplemented with 10% FBS (Giard *et al.*,

1973). Cell viability was confirmed prior to implantation (Vi-Cell Viability Counter, Beckman Coulter, Brea, CA). At 14 days post implantation, mice were injected IP with ~35 µCi $^{18}$F-FDG and returned to their home cage to measure the glycolytic profile of the tumors. After a 50 minute uptake time, the mice were anesthetized with ~2% isoflurane in 100% oxygen, loaded into imaging chambers, and PET imaged for 10 minutes in a Genisys4 system (Sofie Bioscience, Culver City, CA). PET images were generated using a maximum likelihood expectation maximization algorithm, reconstructed with 50 iterations, normalized for detector response, and corrected for isotope decay and photon attenuation. To acquire anatomical complementary images, the PET imaging was followed with a microCT scan (microCT II, Siemens Preclinical Solutions, Knoxville, TN) with a voxel size of 400 um and 200 um, respectively. CT exposure setting were 70 kVp, 500 mAs, 500 ms at 360° rotation in 1° steps with a 2-mm aluminum filtration. CT was reconstructed using a modified Feldkamp process developed by Dr. Richard Taschereau (University of California, Los Angeles).

Tumor $^{18}$F-FDG uptake was calculated as follows using A Medical Image Data Examiner software (AMIDE, v1.0.1., Andy Loening, http://sourceforge.net/projects/amide/): a 2 mm sphere ROI was drawn in the center of the tumor located on CT. Probe uptake was calculated using the following formula:

$SUV_{Tumor} = ROI_{Tumor}$ (Bq ÷ mL) ÷ [injected dose (Bq) * body weight (g)]

As an adjunct measurement of thermography, BAT was collected for histology and routine H&E staining for BAT vacuole quantification. In warm adapted animals, BAT cell cytoplasm is dominated by monolobular lipid droplets and appears to be

morphologically similar to white adipose tissue (Lim *et al.,* 2012). Conversely, BAT cells from cold-adapted animals were foamy and finely vacuolated (Lim *et al.*, 2012). To quantify BAT cell vacuole size, the sections were photographed (DP25, Olympus, Central Valley, PA) 3 times each slide at 40x magnification (BX41, Olympus). Non-BAT tissues, primarily blood vessels, were cropped prior to image processing (Wright Cell Imaging Facility modification of ImageJ, version 1.37c, Wayne Rasband, NIH, http://uhnresearch.com). The images were separated into red, green, and blue channels using a color deconvolution software plugin. To quantitate vacuole size, the green channel was converted to a binary image using the threshold tool, eroded and dilated with a macro to separate the converging vacuole, then pixel size was quantified with the particle analysis tool. The adrenal glands were dissected and weighed.

ΔT BAT and BAT vacuole size were tested for significant differences and interactions by using repeated measures ANOVA to account for multiple sampling from each mouse. Housing group and phenotype (*Prdkc*$^{scid}$ or NU-*Foxn1*$^{nu}$) were each tested as individual factors. Post hoc significance testing was performed and corrected for multiple comparisons by using the Holm–Šidák approach. BAT $^{18}$F-FDG uptake (SUV), tumor weights (mg), tumor $^{18}$F-FDG uptake (SUV), and adrenal weights (mg) were tested by using 2-way ANOVA; housing and *Prdkc*$^{scid}$ or NU-*Foxn1*$^{nu}$ were tested as individual factors, and post-hoc significance testing was performed and corrected for multiple comparisons by using the Holms–Šidák approach. Data sets were tested for homoscedasticity and gross normality to confirm the assumptions of the models were not violated. The α level for all data sets was set to 0.050. All calculations were performed in Stata 12 (version 12.1, StataCorp, College Station, TX). Figures were

created in Prism 6 (version 6.01, GraphPad Software, La Jolla, CA) and are presented as routine box-and-whisker plots, with boxes representing the 25th and 75th percentiles and whiskers representing the minimal and maximal data points.

### b. Results

Qualitatively, we observed with thermography that mice behavioral maintained heated microclimates within the shelters (Figure 3-3 and 3-4). Statistical analysis of longitudinal thermography measurements revealed that housing environment had a significant effect on ΔT BAT ($F_{2,87}$ = 17.89, $P$ < 0.001), accounting for 52% of the total variation, whereas the effect of mouse phenotype (hirsute or nude) was not significant ($F_{1,87}$ = 2.65, $P$ = 0.107). The interaction between housing and phenotype was significant ($F_{2,87}$ = 6.06, $P$ = 0.003), accounting for 11% of the total variation. The day-to-day measurements did not vary significantly ($F_{1,138}$ = 1.04, $P$ = 0.309), indicating consistent measurement practices. *Prdkc*$^{scid}$ mice housed in IVC exhibited greater acute non-shivering thermogenesis compared with those in static cages ($F_{2,87}$ = 9.92, $P$ < 0.001) or IVC with shelters ($F_{2,87}$ = 22.63, $P$ < 0.001). *Prdkc*$^{scid}$ mice in static cages exhibited more ($F_{2,87}$ = 7.87, $P$ < 0.001) acute BAT activation than did those in IVC with shelters. The trend was similar in NU-*Foxn1*$^{nu}$ mice: mice housed in IVC exhibited greater BAT activation than did those in static cages ($F_{2,87}$ =13.18, $P$ < 0.001) or IVC with shelters ($F_{2,87}$ = 17.87, $P$ < 0.001). NU-*Foxn1*$^{nu}$ mice housed in static cages had more BAT activation than did those housed in IVC with shelters ($F_{2,87}$ = 3.96, $P$ = 0.022; Figure 3-4.

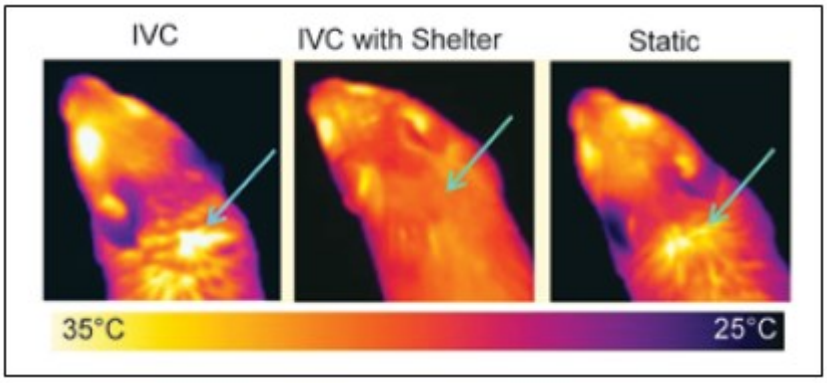


**Figure 3-3** Effect of housing type on non-shivering thermogenesis visualized by thermography in Prkdc$^{scid}$ mice.

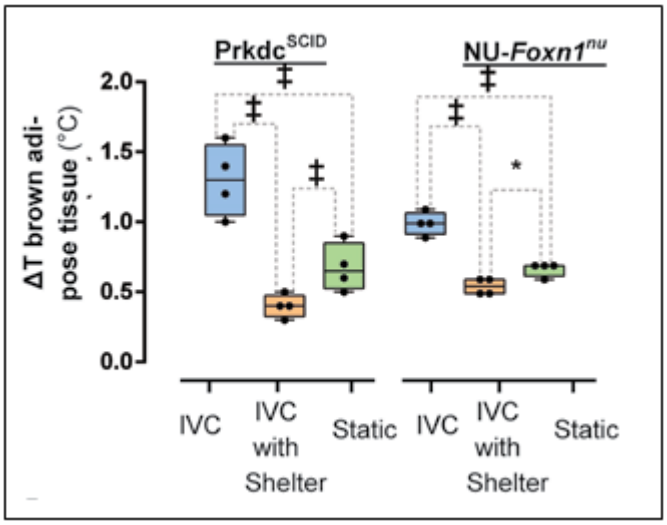


**Figure 3-4** Quantification of non-shivering thermogenesis measured by thermography (ΔT BAT, ºC) in Prkdc$^{scid}$ and NU-*Foxn1*$^{nu}$ male mice (n = 4). *, $P < 0.050$; ‡, $P < 0.001$.

From statistical analysis, 70% of the variation in BAT vacuolation was accounted for by housing conditions ($F_{2,18} = 102.99$, $P < 0.001$) and 7% by mouse phenotype ($F_{1,18} = 21.21$, $P < 0.001$). The interaction was significant ($F_{2,18} = 23.93$, $P < 0.001$), accounting for 16% of the total variation. On post-hoc analysis, *Prdkc*$^{scid}$ mice housed in IVC with shelters had smaller ($F_{2,18} = 5.26$, $P = 0.016$) vacuoles than did mice housed in static cages (Figure 3-5 and 3-6). NU-*Foxn1*$^{nu}$ mice housed in IVC or IVC with shelters had smaller ($F_{2,18} = 18.05$, $P < 0.001$) vacuoles than those housed in static

cages, but there was no significant difference between mice housed in IVC and those in IVC with shelters ($F_{2,18}$ = 0.42, $P$ = 0.662; Figure 3-6). The histologic analysis demonstrates greater chronic activation of BAT in mice housed in IVC compared with static cages and that 3-wk exposure to shelters partially rescues this effect in *Prdkc*$^{scid}$ but not NU-*Foxn1*$^{nu}$ mice (Figure 3-5 and 3-6).

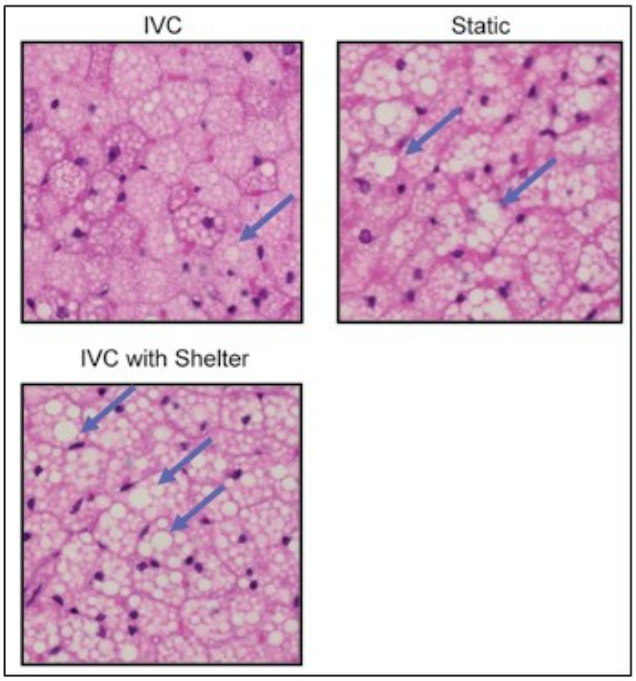


**Figure 3-5** Effect of housing type on brown adipose tissue vacuole size (arrows) in Prkdc$^{scid}$ male mice (n = 4 per group) as visualized by H&E histology.

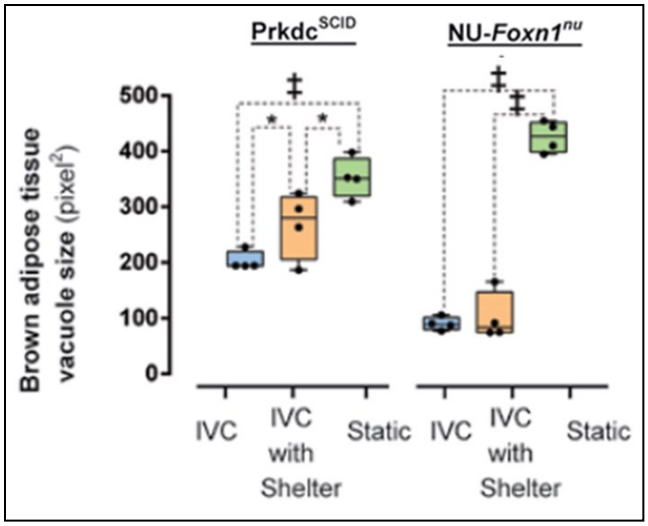


**Figure 3-6** Quantification of BAT vacuole size by housing type in in Prkdc$^{scid}$ and NU-*Foxn1*$^{nu}$ male mice (n = 4 per group). *, $P < 0.050$; ‡, $P < 0.001$.

Using the previously described relationship between ΔT BAT and EPR (David *et al.*, 2013a), murine EPR increased by 18.9%, SD 0.2 and 48.3%, SD 0.6 in hirsute and nude mice, respectively, housed in IVC compared to static cages.

The gross weight of subcutaneous tumors varied by housing type ($F_{2,18} = 33.43$, $P < 0.001$) and mouse phenotype ($F_{1,18} = 22.57$, $P < 0.001$), accounting for 54% and 18% of the total variance, respectively. The interaction of these parameters was significant ($F_{2,18} = 8.46$, $P < 0.001$), accounting for 14% of the total variance. Subcutaneous tumors at 14 d after implantation were smaller in *Prdkc*$^{scid}$ mice housed in IVC compared with static cages ($F_{2,18} = 4.55$, $P = 0.025$) but did not differ from those of mice housed in IVC with shelters ($F_{2,18} = 3.48$, $P = 0.053$; Figure 3-7).

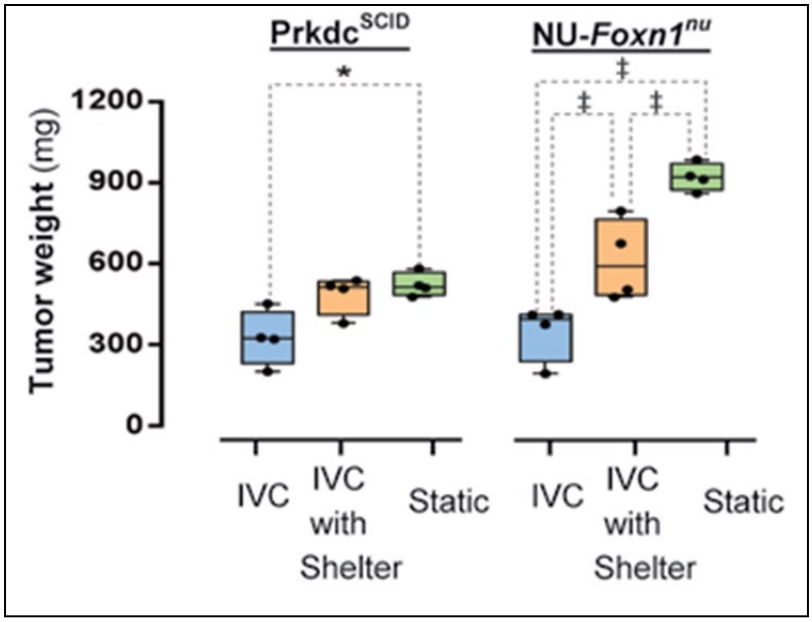


**Figure 3-7** The effect of ventilated caging and shelters on subcutaneous epitheloid carcinoma growth (A431) at 14 days post-implantation in Prdkc$^{scid}$ and NU-*Foxn1*$^{nu}$ mice housed in IVC, IVC with shelters, and static cages (n = 4 per group). *, $P < 0.050$; ‡, $P < 0.001$

Tumor $^{18}$F-FDG was effected by housing type ($F_{2,18} = 35.50$, $P < 0.001$), accounting for 76% of the total variance, while mouse phenotype did not alter tumor $^{18}$F-FDG uptake ($F_{1,18} = 2.33$, $P = 0.144$). The interaction was not significant ($F_{2,18} = 0.91$, $p = 0.420$). Tumor $^{18}$F-FDG uptake in PET scans in Prdkc$^{scid}$ mice housed in IVC was significantly lower than that of mice housed in static cages ($F_{2,18} = 18.17$, $P < 0.001$) but not IVC with shelters ($F_{2,18} = 0.21$, $P = 0.814$; Figure 3-8 and 3-9). Prdkc$^{scid}$ mice housed in IVC with shelters had significantly ($F_{2,18} = 8.513$, $P = 0.003$) lower uptake in tumors than did those in housed in static cages. $^{18}$F-FDG uptake of tumors in NU-*Foxn1*$^{nu}$ mice housed in IVC was lower than that of tumors implanted in mice housed in static cages ($F_{2,18} = 9.68$, $P = 0.001$) but not IVC with shelters ($F_{2,18} = 0.14$, $P = 0.869$; Figure 3-9). Tumors in NU-*Foxn1*$^{nu}$ mice housed in IVC with shelters had significantly

($F_{2,18}$ = 7.21, $P$ =0.004) lower 18F-FDG uptake than did mice housed in static cages (Figure 3-9).

The PET quantification demonstrates that there is a significant difference in tumor glycolytic metabolism between mice housed in IVC compared with static cages. During the uptake period, we observed that the mice were very active after injection and that the animals did not return to the shelters for 25, SD 7 min (mean +/- 1 SD; Prdkc$^{scid}$ mice) or 29, SD 6 min (NU-*Foxn1*$^{nu}$) after injection, well after the peak tumor uptake time (Fueger *et al.*, 2006).

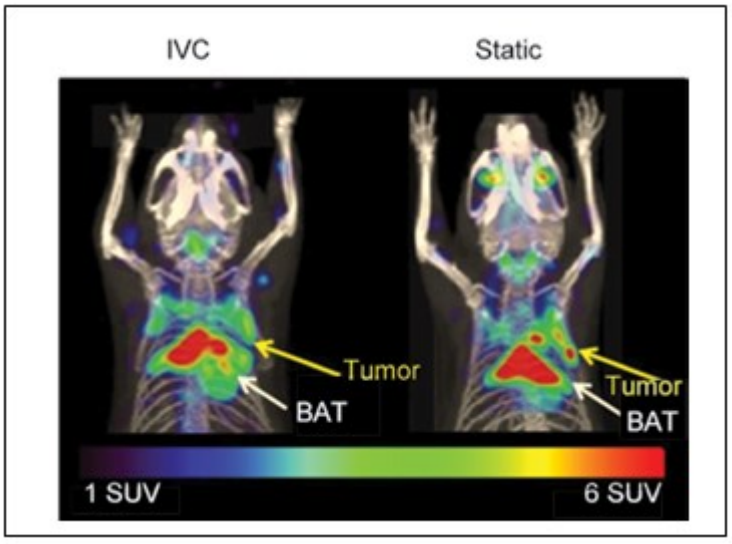


**Figure 3-8** Effect of housing type on subcutaneous epitheloid carcinomas (A431, yellow arrow) glycolytic metabolism visualized by $^{18}$F-FDG PET/CT imaging in Prkdc$^{Scid}$ mice. Images were produced using maximal intensity projection (25-mm slices).

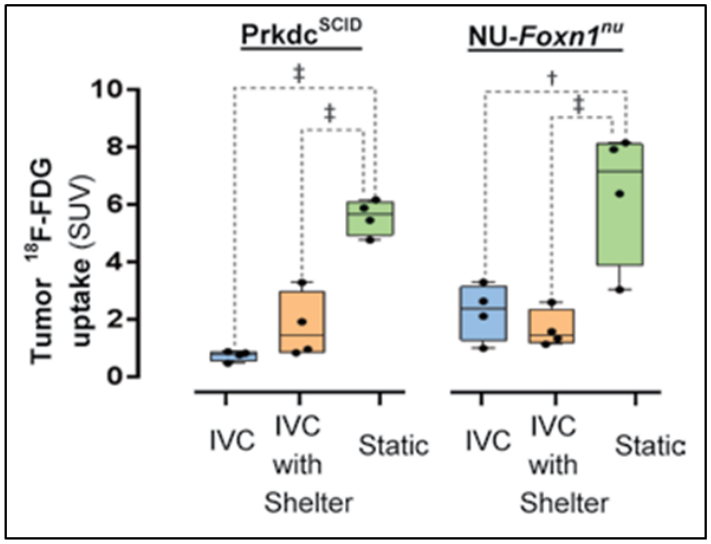


**Figure 3-9** Quantification of the glycolytic metabolism of subcutaneous epitheloid carcinomas (A431) using $^{18}$F-FDG PET imaging (n = 4 per group). ‡, $P < 0.001$.

Adrenal size was significantly affected by housing condition ($F_{2,18} = 35.50$, $P < 0.001$) and mouse phenotype ($F_{1,18} = 9.16$, $P = 0.007$), accounting for 63% and 10% of the total variance, respectively. It is unclear if the adrenal size was induced by larger

tumor burden or the cold-stress associated with IVCs. The statistical interaction of housing condition and phenotype was not significant ($F_{2,18}$ = 3.34, $P$ = 0.058). Adrenal weights were greater in *Prdkc*$^{scid}$ mice housed in IVC compared to IVC with shelters ($F_{2,18}$ = 8.95, $P$ < 0.001) or static cages ($F_{2,18}$ = 23.34, $P$ < 0.001). Adrenal weights of *Prdkc*$^{scid}$ mice housed in IVC with shelters did not differ from those of mice housed in static cages ($F_{2,18}$ = 0.19, $P$ = 0.831). The adrenal weights of NU-*Foxn1*$^{nu}$ mice housed in IVC were greater than that of those housed in static cages ($F_{2,18}$ = 4.51, $P$ = 0.030) but not IVC with shelters ($F_{2,18}$ = 3.03, $P$ = 0.074). Adrenal weights in NU-*Foxn1*$^{nu}$ mice did not differ ($F_{2,18}$ = 0.19, $P$ = 0.831) between those housed in IVC with shelters compared with static cages (Figure 3-10).

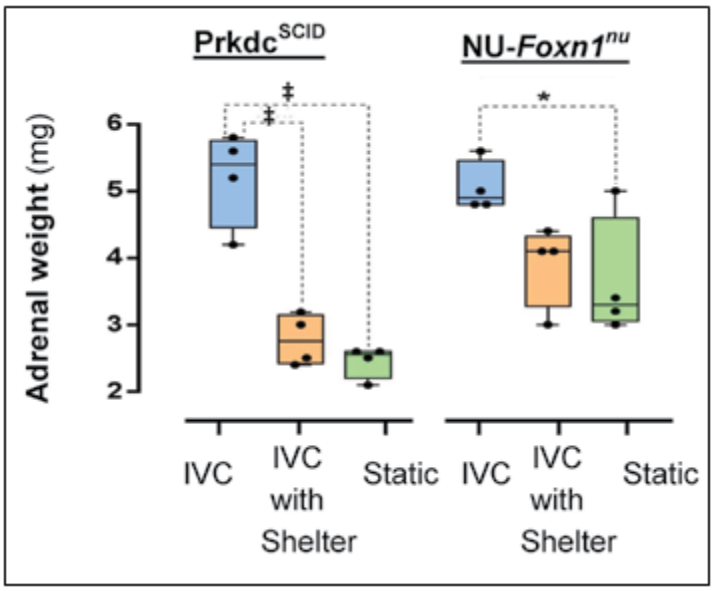


**Figure 3-10** Effect of housing type on adrenal gross weight. Gross adrenal weights of Prkdc$^{scid}$ and NU-*Foxn1*$^{nu}$ mice housed in IVC, IVC with shelters, and static cages (n = 4 per group). *, $P$ < 0.050; ‡, $P$ < 0.001.

### c. Discussion

Our data is consistent with the hypothesis that mice are under significantly greater cold-stress when housed in IVCs: mice housed in IVC express greater acute non-

shivering thermogenesis and exhibit smaller BAT vacuoles (indicating chronic BAT activation as seen in cold-adapted animals; Lim *et al.*, 2012). In addition to the physiologic consequences of IVC, subcutaneously tumors were smaller and had reduced glycolytic metabolism when implanted in both *Prdkc*$^{scid}$ and NU-*Foxn1*$^{nu}$ mice housed in IVC compared to housing in static cages. In light of the BAT activation we observed in the current study and previous reports of cold sensitivity in subcutaneous tumors, (Fueger *et al.*, 2006) our data is consistent with the hypothesis that housing-dependent cold stress blunts tumor growth. These findings have implications for investigators in numerous fields, including metabolism, oncology, and endocrinology.

Mice housed in IVC have grossly enlarged adrenal glands compared to mice housed in static cages. Although neuroendocrine metrics were beyond the scope of the study design, the enlarged adrenal glands we observed are consistent with previously described cold-mediated hypothalamic activation, with subsequent sympathetic cascades associated with non-shivering thermogenesis in $\beta_3$-receptor–rich BAT (Harvey and Sutcliffe, 2010; Morrison *et al.*, 2008). This mechanism is well conserved among mammals and occurs in multiple species, including rodents and humans (Morrison *et al.*, 2008). However, we did not investigate the mechanism and cannot rule out other explanations, such as vibration or ultrasonic noise, which are also known to induce stress in mice (Reynolds *et al.*, 2010).

We postulate the calculated 18.9% +/- 0.2% and 48.3% +/- 0.6% increase in EPR in hirsute and nude mice, respectively, is driven by the cooling effects of 0.2 m/s air drafts. The direction and magnitude was expected based on the 0.2 m/s air speed within the IVC and Chappell and Holsclaw's observation that oxygen consumption (ml/g per min)

in eastern Californian deer mice (*Peromyscus maniculatus sonoriensis*, mean weight 21.3 g) increased significantly at low air speeds (see Figure 3-2). Moreover the observation that shelters that block drafts ablated the additional cold-stress (Figure 3-3 and 3-4) is consistent with the hypothesis that air drafts are a source of cold-stress.

14 days post-injection, the tumors were significantly smaller and had significantly reduced $^{18}$F-FDG PET uptake in mice housed in IVC compared to the mice housed in static cages. The growth retardation was significantly, but only partially, rescued by the addition of shelters in the IVC in nude mice and insignificantly trended towards rescue in SCID mice. Shelters did not rescue the IVC associated decrease in glucose uptake on $^{18}$F-FDG PET. We believe this finding is due to the observer effect, an artifact created by experimental manipulation: rodents exhibit a hyperthermic response to handling (Rudaya *et al.*, 2005). We transiently reduced the cold stress imposed by IVC by handling the animals prior to the experiment and reduced metabolic activity in BAT (Fueger *et al.*, 2006). Despite the technical challenges of assaying cold-stress by administrating $^{18}$F-FDG via injection that excites the mouse (Romanovsky *et al.*, 1998) the data reveals a very important finding: the growth and glycolytic metabolism of subcutaneous tumors varies by house type. This observation also highlights the transient nature of non-shivering thermogenesis and potential difficulty in measuring BAT metabolism using PET.

We speculate that the mechanism of shelter-associated rescue of cold-stress in our study reflects the combined effects of an area free of air flow and the increased retention of radiated heat in a 3D insulator. These results highlight the importance that behaviorally maintained heated microclimates play in the homeostasis of murine

physiology and, in turn, experimental results. Allowing mice to behaviorally thermoregulate in IVC reduces the physiology stress and benefits scientists by improving the uniformity in physiological states and experimental results across housing systems (at least, in the context of ubiquitous subcutaneous tumor models). In addition this work illustrates that shelters are a simple yet substantial refinement to IVC housing.

## III. Quantifying cold-stress variations across different IVC systems

### a. Background

In the data presented above, we reported that mice housed in one ventilated system (InnoRack, Innovive) exhibited significantly more non-shivering thermogenesis, a metric of cold-stress (David *et al.*, 2013a), than mice housed in static cages (David *et al.*, 2013b). Each vendor manufactures IVCs with different specifications, such as air changes per hour, airflow pattern, and air velocity (Milite, 2008). We hypothesize that mice housed in different IVC systems will experience different degrees of cold-stress. In this aim, we will measure cold-stress in mice housed in two IVC designs.

### b. Methods

8-week old Swiss-Webster female mice were group housed (3 mice per cage) in one of two IVC systems and two static cages used on UCLA's campus: SuperMouse with 35 air changes per hour at 0.2 meters per second (Lab Products, Seaford, DE), InnoRack with 60 air changes per hour at 0.2 meters per second (Innovive, San Diego, CA), static polycarbonate cages (Lab Products), or polyethylene static cages (Innovive; n = 12 per group, 36 mice balanced across each housing type). The cages were lined with ~200 gram of bedding (corncob in the Innovive caging; beta-chip in the Lab Product

cages) with a 1 square inch cotton nestlet (standard enrichment). Non-shivering thermogenesis was measured by thermography as previously described (David *et al.*, 2013a) between the hours of 09:00-10:00 to control for circadian rhythm (Sutton *et al.*, 2012). Group size was determined by *a priori* F family test power analysis with the following parameters derived from our pilot studies: effect size f 0.37, α 0.05, and 0.95 power (G*Power 3.1.5, Franz Faul, 2013, Universitat Keil, Germany). The data were analyzed by two-way ANOVA with the factors caging type (static and IVC) and vendor (Lab Products, Seaford, DE and Innovive, San Diego, CA) with post-hoc significance testing with a Holm-Sidak correction. Significance cutoff was set to α = 0.05. Data sets were tested for homoscedasticity and gross normality to confirm the assumptions of the models were not violated. The graph was created in GraphPad Prism 6 (GraphPad Software, La Jolla, CA).

c. **Results**

Non-shivering thermogenesis as measured by thermography significantly differed between mice housed in static cages and IVC ($F_{1,44}$ = 31.97; $P$ < 0.010; Figure 3-11). Cold-stress experienced by mice housed in IVC of either design did not significantly vary ($F_{1,44}$ = 0.002; $P$ = 0.967): non-shivering thermogenesis as measured by ΔT BAT in Lab Products' IVC averaged 1.217, SD 0.482 ºC compared to Innovive design average of 1.200, SD 0.226 ºC (Figure 3-11). Cold-stress of mice housed in static cages of either design also did not significantly vary ($P$ = 0.498): non-shivering thermogenesis as measured by ΔT BAT in Lab Products' static averaged 0.6ºC, SD 0.4 compared to Innovive design average of 0.7 ºC, SD 0.1 (Figure 3-11).

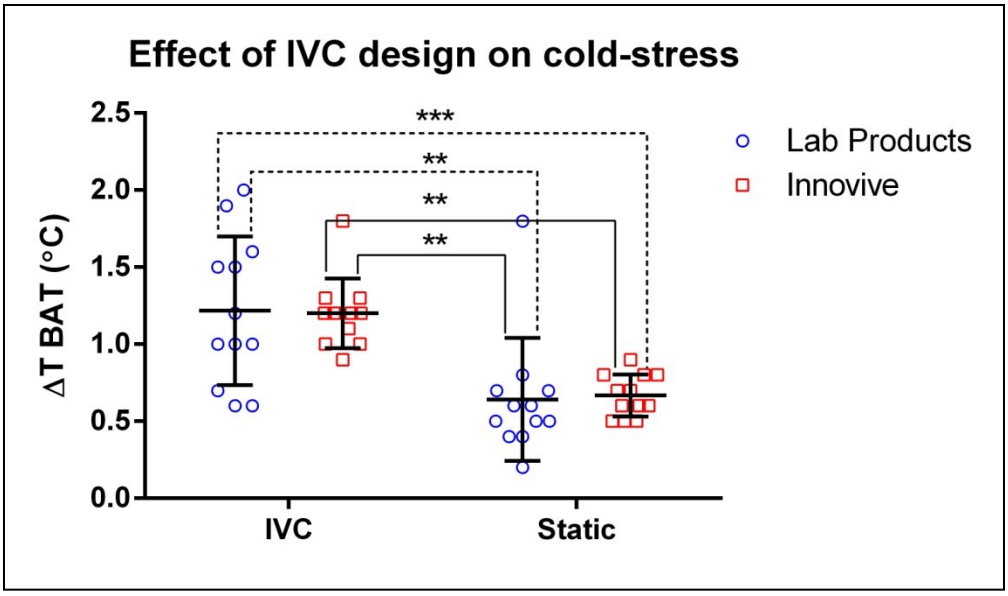


**Figure 3-11**. Effect of caging design on cold-stress as measured by thermography (n = 12 SW female mice per group). Error bars represent standard deviation. **, $P < 0.010$; ***, $P < 0.001$

d. **Discussion**

Cold-stress as measured by non-shivering thermogenesis did not significantly vary by IVC design type despite the lower ACH (35 compared to 60 of the Innovive) of the Lab Product's IVC. Within the context these two common designs, the author rejects the hypothesis that IVC design alters cold-stress suggesting the direct draft exposure is the more relevant metric to investigate. It is unclear if the direct contact of air drafts (reported to be 0.2 m/s in both designs) or the mass air removal and subsequent inability to maintain heated micro-climates is the primary driver of thermal energy loss in mice. Interestingly, cold-stress did not significantly vary between the static cages of thicker polycarbonate with beta-chip bedding and thinner polyethylene with corncob bedding.

## IV. Establishing stocking density effects for IVC housing

### a. Background

The *Guide for the Care and Use of Laboratory Animals* recommends social housing of animals (NRC, 2011). However, the optimal standards of murine stocking density (the number of animals per cage) are largely unexplored. The limited studies published to date are in static systems (Gordon, 2012) and have little bearing to the increased number of mice often housed in IVCs. The studies on IVCs have focused primarily on waste gas management (Milite, 2008) and have neglected to investigate possible cold-stress associated with IVCs.

The most common social activity of mice is huddling (Arakawa *et al.*, 2007; Harshaw and Alberts, 2012). Social huddling is an important thermoregulatory behavior of mice that reduces group surface area (Batchedler *et al*., 1982) and reduces thermal preference by ~1ºC (Gaskill *et al.*, 2009; Gordon *et al.*, 1998). Huddling is the most frequent and, by implication, the most important social activity of mice (Arakawa *et al.*, 2007). Thus, thermoregulatory metrics are likely the best measure of stocking density optimization.

In this experiment, we seek to establish the minimum ideal stocking density based on physiological performance data. We housed mice at various stocking densities, quantitating behavioral-thermoregulation, and used regression modeling to establish the optimum stocking density for laboratory mice housed in modern IVC.

### b. Methods

To evaluate the cold-stress alleviating benefits of huddling, mice were housed in IVCs (Innovive, San Diego, CA) with ~200 grams of corncob bedding with a 1 square

inch cotton nestlet (standard enrichment). Each mouse was housed at a stocking densities of 5 (the maximum regulatory allowed; NRC, 2011), 4, 3, 2, or 1 with 72 hours of acclimation between each stocking density. To represent the spectrum of mouse phenotypes and behaviors, we will used the following 2x2x2 factorial designs: male and female mice, with females having higher propensity to huddle (Batchelder *et al.*, 1983); hirsute (furred) and nude mice, with hirsute mice experiencing less cold-stress than nudes (David *et al.*, 2013a); and C57BL/J (C57BL/J, B6.Cg-*Foxn1*nu/J) and BALB/C (BALB/C, NU-*Foxn1*) mice, with C57BL/J having higher propensity to huddle (An *et al.*, 2011; n = 5 per gender per strain per phenotype as defined as hirsute or nude, for a total of 40 mice balanced across groups). To measure cold-stress, non-shivering thermogenesis was quantified with thermography via a previously establish protocol (David *et al.*, 2013a) twice per day between 09:00-10:00 and 14:00-15:00. Group size was determined by *a priori* F family test power analysis using $\alpha = 0.05$, power 0.90, and effect size 0.37 based on pilot data (G*Power 3.1.5, Franz Faul, 2012, Universitat Keil, Germany). To minimize fighting, nestlets were transferred with the mice and males were handled prior to females.

Significance of each factor (stocking density, gender, strain, and phenotype) was tested against non-shivering thermogenesis (the dependent variable) using a generalized, repeat measures linear mixed effects model (R, R Studio, Boston, MA). Time of day (morning or afternoon) did not significantly alter non-shivering thermogenesis ($P = 0.784$) and was removed from the analysis. Each level of stocking density was compared by post-hoc contrast with a Holm-Sidak correction (R, R Studio, Boston, MA). Significance cutoff was set to $\alpha = 0.050$. Linearity was confirmed post-

hoc ($P < 0.001$) to ensure the correct model was applied to the data. Data sets were tested for homoscedasticity and gross normality to confirm the assumptions of the models were not violated. Graphs were created in GraphPad Prism 6 (GraphPad Software, La Jolla, CA).

c. **Results**

Stocking density significantly affected non-shivering thermogenesis (Figure 3-12). On post-hoc analysis, stocking densities of 2 through 5 improved cold-stress over single housing, and stocking densities of 3 through 5 improved cold-stress over stocking density of 2 (Figure 3-12). Stocking densities of 3 through 5 were not significantly different from one another (Figure 3-12). Gender did not significantly influence non-shivering thermogenesis values ($P = 0.415$).

The nude phenotype was significantly more cold-stressed than the hirsute mice ($P < 0.001$); nude mice exhibited an average of 0.380, SE 0.049 greater ΔT BAT (ºC) than hirsuite. BALB/c mice, the poor huddlers, were significantly more cold-stressed than C57BL/6 mice ($P = 0.003$), exhibiting an average of 0.145, SE 0.048 greater ΔT BAT (ºC) than C57BL/6 mice.

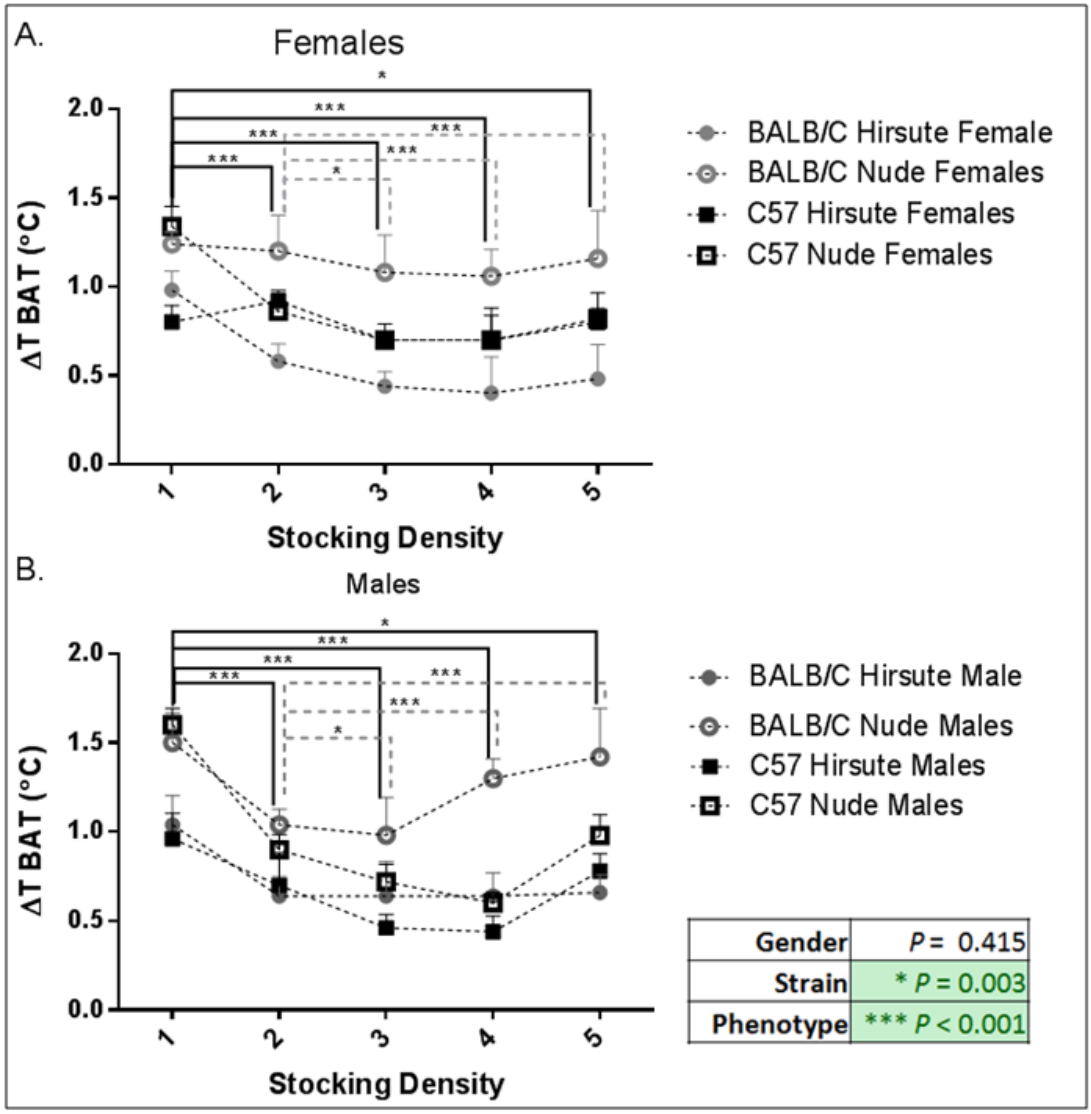


**Figure 3-12**. Effect of stocking density on non-shivering thermogenesis measured by thermography in (A) female and (B) male, nude and hirsute, BALB/c and C57BL/6 mice. (n = 5 per group). Non-shivering thermogenesis significantly decreases from stocking density of 1 to 2 and 2 to 3, but no more with additional mice. Hirsute and C57BL/6 exhibit less non-shivering thermogenesis than nude and BABL/c mice, respectively. Gender was not significant. Error bar represent standard error. *, $P < 0.050$; ***, $P < 0.001$

d. **Discussion**

Increasing stocking density up to 3 animals per cage significantly reduced cold-stress in mice. Based on these results, the author recommends a minimum stocking density of 3 mice per cage.

The reduction in non-shivering thermogenesis associated with high stocking density is incomplete compared with the reductions observed at thermoneutrality (David *et al.*, 2013a). Thus, further improvements in cold-stress reduction are still possible through nesting material (Gaskill *et al.*, 2012), engineering controls (see Chapter 4), or raising the environmental temperature (Chappell and Holsclaw, 1984).

Environmental enrichment studies, such as this one, are often criticized for their limited scope: they often apply only to a particular strain, are narrowly tailored to environments that have little bearing to vivarium conditions, etc. (Toth *et al.*, 2011). Moreover, the findings and conclusions cannot be broadly applied because metrics used in many studies have poorly defined benefits to mouse welfare and the implications of experiment results are unknown (Toth *et al.*, 2011).

The goal of this study was to develop the most broadly applicable recommendations as possible. The study was designed to capture the diversity of murine behaviors and phenotypes using a complete factorial design: BABL/c, poor huddlers, and C57BL/6, relatively good huddlers (An *et al.*, 2013); male and females; and hirsute and nude mice, an extreme but common phenotype that is more prone to cold-stress (David *et al.*, 2013a). Thus, the conclusions present here should apply to the vast majority of laboratory mice.

# Chapter 4: Development and Validation of Novel Individually Ventilated Caging Systems

This chapter is based on the following works:

**David JM,** Stout DB. 2013. US 61,895,885 (provisional): Device, System, and Method for Measuring and Reducing Cold Stress of Housed Laboratory Animals. Washington, DC: U.S. Patent and Trademark Office.

## I. Novel engineering control to minimize cold-stress on mice

IVC impose cold-stress on mice (Chapter 3). This cold-stress alters experimental results, leading to potential experimental irreproducibility (David *et al.*, 2013b). However, IVC possess many desirable characteristics: high stocking density per square footage of vivarium space, reduced waste gas accumulation (Hoglund and Renstrom, 2000), excellent murine and experimental pathogen control (Brielemier *et al.*, 2006; Compton *et al.*, 2004), lower allergen exposure to staff (Reeb-Whitaker *et al.*, 1999), and prolonged cage change interval (from 1 to 2 weeks). Prolonged cage change interval is especially important because it is stressful for mice (Rasmussen *et al.*, 2011) and labor intensive (Milite, 2008). All of these benefits depend on the high rate of air changes per hour to remove waste gases.

### a. Air flow patterns

IVC airflow patterns vary greatly between vendors. Generally, the three most common approaches are the following: (1) supplying air through the lid, passing under a suspended object in the middle of the cage (i.e. the food hopper and/or the water bottle), and exhausted through the lid, creating a “U” shape pattern (Conger *et al.*, 2011); (2) supply air at the animal level, traversing the entire cage length at the animal level, and exhausting via the lid top (Garbriel *et al.*, 2013); or (3) supply air at the top of the cage, traveling the length of the cage, diverting downwards towards the animal, and exhausting in the top of the cage near the supply port (Jae-Jin, 2002).

In this chapter, we describe a novel modification to minimize the effects of air drafts on mice while simultaneously maintaining the benefits of IVC, namely the 2 week

cage change interval. The concept of the design is to provide a draft-free region for the mice to nest while maintaining the same ACH. We hypothesize this design will simultaneously decrease cold-stress and maintain sanitary condition that will facilitate the 2 week cage change interval.

We have designed and filed a provisional patent on a novel IVC with no drafts over the nesting area (David and Stout, 2013). We speculate this will reduce cold-stress because of the following aspects of murine behavior and physiology:

(1) drafts, even small ones (e.g. 0.25 m/s), induce physiological stress (Figures 3-1, 3-2, and 3-3; Chappell and Holsclaw, 1984);
(2) mice are most vulnerable to cold-stress during the light cycle when they are largely immobile (Figure 2-11; Gordon, 2012); and
(3) mice spend the bulk of the light cycle in their nesting area.

We chose to focus on the "U" shape pattern because it is one the most germane to our facility. Any novel design elements are expected to be compatible with existing ventilated racks.

## II. Novel draft design reduces cold-stress

### a. *In silco* computed fluid dynamic simulations

To simulate air flow patterns in a modern IVC with a "U" shaped air flow (Figure 4-1) and the novel draft-free nesting regions (Figure 4-2) of the cage, IVC air flow was modeled *in silco* (SolidWorks® 2013, Dassault systemes) using a computed fluid dynamic plugin (Flow Simulation, Dassault systemes). The computed fluid dynamic

simulations were run with the following parameters based on blower settings: a constant 60 ACH with a cage volume of 6.6 liters.

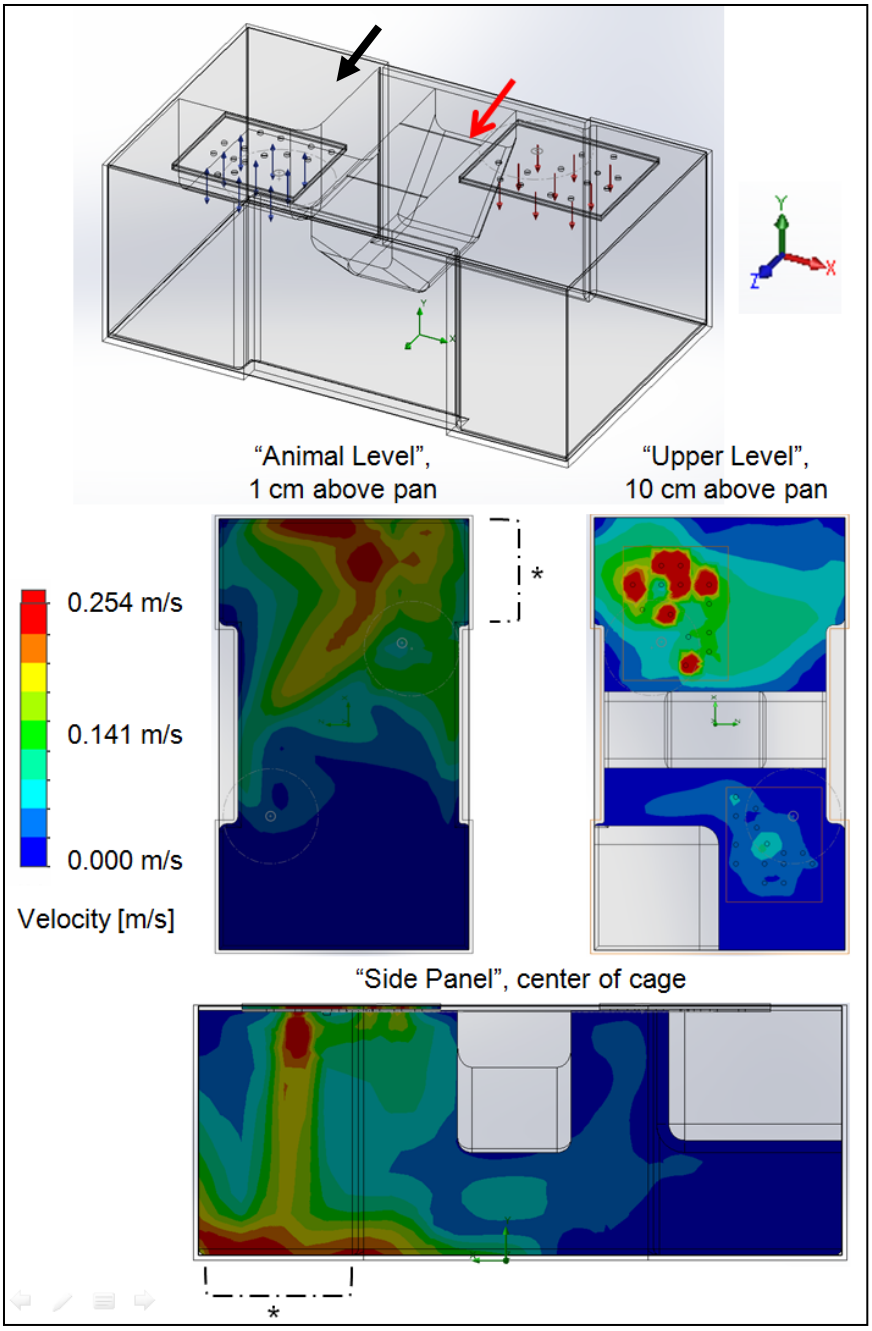


**Figure 4-1** A modern IVC (Innovive, San Deigo, CA) with a "U" shaped air flow pattern was modeled *in silico*. The following features were included in the computed fluid dynamics simulations: feed hopper (red arrow), water bottle holder (black arrow), air supply diffuser plate, and exhaust plate. Air flow patterns were modeled with computed fluid dynamic simulations (Flow Simulation, Dassault systems). Slice air velocity maps are presented here: the "animal level", 1 cm above the interior cage pan; "upper level", 10 cm about the pan base; and "side panel", length central slice. The most common nesting area of the mice ("*") is located in the rear of the cage, which is typically the darkest region.

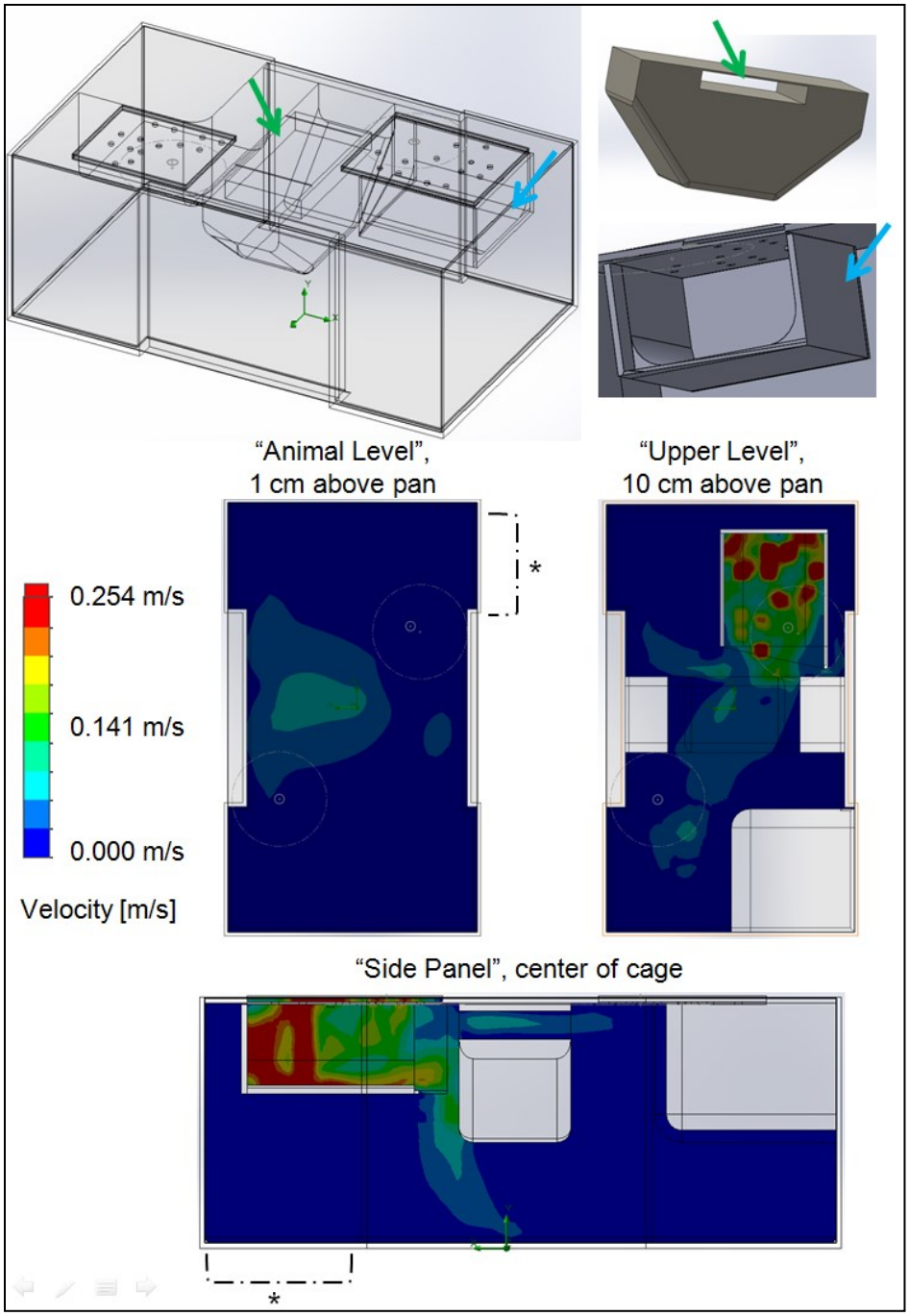


**Figure 4-2** The novel, low draft IVC was modeled *in silico.* The following features were included in the computed fluid dynamic simulations: feed hopper, water bottle holder, air supply diffuser plate, exhaust plate, a draft diversion channel in the hopper (green arrow), and a deflector box (blue arrow). Air flow patterns were modeled with computed fluid dynamic simulations (Flow Simulation, Dassault systems). Slice air velocity maps are presented here: the "animal level", 1 cm above the interior cage pan; "upper level", 10 cm about the pan base; and "side panel", length central slice. The most common nesting area of the mice ("*") is located in the rear of the cage, which is typically the darkest region.

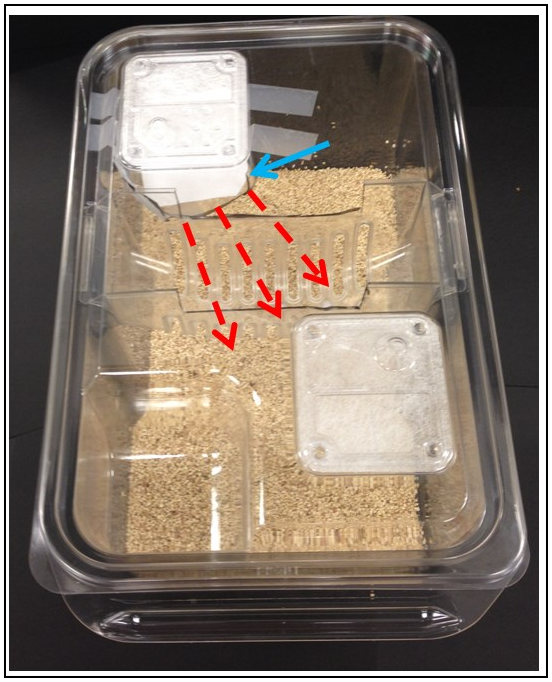

**Figure 4-3** A photograph of a prototype of the novel, low draft IVC with the air current deflection box (blue arrow) and the air flow path through the high channel through the hopper (red arrows).

b. ***In vivo* validation**

i. **Background**

To validate the *in silico* simulations, cold-stress was measured in mice housed in classic IVC and novel, low-draft IVC housing (Figure 4-3).

ii. **Methods**

To quantitate the potential reduction in cold-stress of mice housed in the novel, low-draft IVC, adult C57BL/6 female mice were housed in the novel, low-draft housing (Figure 4-2) or the classic IVC (Figure 4-1; Innovive, San Diego, CA) at a stocking density of 3 (n = 15, randomized order, cross-over study design). Each animal was marked for identification. Rack position was maintained during cross-over to control for factors such as lighting, proximity to the door, etc. The mice were acclimated for 72 hours to each cage environment prior to data acquisition. Social groups were

maintained throughout the experiment to avoid fighting. Non-thermogenesis was measured via thermography between 09:00 and 10:00 to control for circadian rhythm (Sutton *et al.*, 2012) using a previously establish method (David *et al*, 2013a).

Group size was determined by *a priori* F test family power analysis based on pilot studies using the parameters: effect size f 0.37, α 0.05, and 0.95 power (G*Power 3.1.5, Franz Faul, 2013, Universitat Keli, Germany).

Non-shivering thermogenesis of each mouse was compared to itself in each IVC type by a paired, two-tail T-test. Significance cutoff was set to 0.050. Results are presented as individual residue plot (Prism 6, GraphPad Software, San Deigo, CA), where each data point represents the ΔT BAT measured in the novel, low draft design minus the ΔT BAT measured in the classic IVC. Values below 0 represent less non-shivering thermogenesis in the novel, low draft IVC and vise versa.

### iii. **Results**

Mice housed in the novel, low-draft IVC (ΔT BAT = 0.820ºC, SE 0.207) exhibited significantly less non-shivering thermogenesis than mice housed in the classic IVC (ΔT BAT = 1.080 ºC, SE 0.173; *P* = 0.004). The mean difference between the housing was 0.260°C, SE 0.077

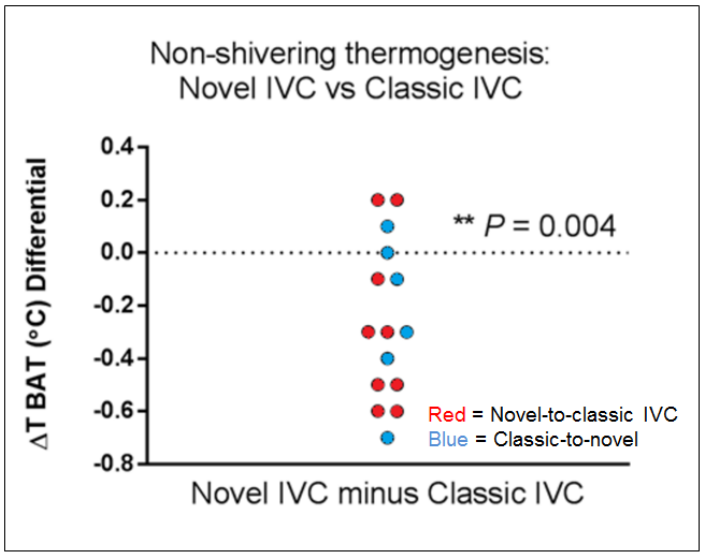


**Figure 4-4** Effect of novel IVC design on cold-stress. Residue plot of differential non-shivering thermogenesis (ΔT BAT, °C) as measured by thermography in female C57BL/6 mice (n=15) at a stocking density of 3. Mice housed in novel, low-draft IVC exhibit significantly less non-shivering thermogenesis compared to classic IVC design. **, $P = 0.004$

### iv. **Discussion**

The novel, low-draft IVC design was associated with significantly less cold-stress than the classic IVC. These results suggest the direct drafts rather than the high ACH is the primary source of cold-stress in the IVC, which was unclear from the previous experiments (Chapter 3).

These promising results should not be confused with alleviating all cold-stress from laboratory mice. This design only addresses the additional cold-stress associated with IVC that is above and beyond that of the vivarium temperature issue. Additional nesting material, shelter, and/or rises in the environmental temperature would be required to alleviate the environmental induced cold-stress. Moreover, the magnitude of cold-stress reduction associated with the novel, low draft IVC (Figure 4-4) is less than static cages (Figure 3-11) at the same stocking density (3 mice per cage). This

suggests the novel design grants a partial rescue of cold-stress associated with IVCs and further improvements are possible.

This novel engineering control should be appealing to vivarium managers because it is backwards compatible with current ventilated racks, economically viable, conforms with current husbandry SOPs, and there is no additional labor to the cage change process. In summary, this novel cage can be implemented with minimal fiscal or labor costs.

An alternative approach to alleviating cold-stress associated with IVC would be to raise the environmental temperature. Chappell and Holsclaw made the observation that oxygen consumption of mice increases when exposed to relatively mild drafts (0.25 m/s); the draft-induced increase in oxygen consumption could be ablated by raising the temperature of the air (1984).

### c. **Micro-environmental ammonia**

#### i. **Background**

The two week cage change interval is one of the most important advantages of IVC over static cages changed weekly because the event is stressful for mice (Rasmussen *et al.*, 2011) and labor intensive (Milite, 2008). Any novel design must maintain the 2 week cage change interval to ensure adoption and require minimal additional labor time or expense.

Gaseous ammonia is the primary determinant of change interval, both for animal and human comfort. The earliest ammonia induced pathology is olfactory epithelial degeneration (Vogelwied *et al.*, 2011). Olfactory epithelial degeneration has been

observed at a time-weighted average of 50.6 ppm in static cages at day 8 post cage change (CD-1 mice at stocking density 4 per cage; Vogelwied *et al.*, 2011). Federal industrial hygiene standards limit human exposure to time weighted average of 25 ppm over 8 hours or short-term exposures of 35 ppm (OSHA, 1997). Based on the OSHA recommendations for humans, and the lack of any specified exposure level in the *Guide* (NRC, 2011), we have selected a cut off time weighted average of 25 ppm as our upper limit for ammonia exposure.

ii. **Method**

Sealed sampling ports were created over the nesting area in the novel, low-draft IVC and classic IVC (Innovive, San Diego, CA) using a hole punch. Male, adult C57BL/6 mice were housed in the novel, low-draft IVC or classic IVC (3 mice per cage) on ~200 grams of corncob bedding with a 1 square inch cotton nestlet (n = 3 cages per group * 3 mice per cage, 18 total mice balanced across groups). On day 0 (baseline), 7, and 14, time weighted average ammonia concentrations was assayed using dosimeter tubes (Ammonia Time Weighted Average Dosimeter Tube, Sensidyne, St. Petersburg, FL, range 5-200 ppm $NH_3$) for 32 minutes at 120 mL/minute using a vacuum-pressure pump (Barnant Col, Carrinton, IL). Ammonia concentration was calculated per the manufacturer's instructions to achieve the equivalent of 8 hour time weighted average (http://www.zefon.com/analytical/download/stubes/501.pdf):

Time Weight Average ($NH_3$ ppm) = I x 3840 mL/V

I = Scale Reading

V = Sample air volume mL [Flow rate (mL/min) x sampling duration (min)]

The calculated ammonia concentration of each caging type was compared by two-way ANOVA with the following factors: IVC design (novel and classic) and time point (day 0, 7, and 14). Significance of each point was determined by post-hoc test with a Holm-Sidak correction. Significance was cut off was set to $\alpha = 0.050$. Ammonia concentrations below the level of detection of the dosimeter (5 ppm) were assumed to be 0 ppm for calculation purposes.

### iii. **Results**

Ammonia concentrations in both designs were below the detection limitations of the dosimeter tubes at day 0 and 7 days post cage change. On day 14, the novel, low-draft IVC had significantly higher ammonia concentrations (7 ppm, SD 2.5) than the classic IVC (below detection; $P < 0.001$; Figure 4-5). Time and IVC design significantly interacted ($F_{2,12} = 25.474$, $P < 0.001$), accounting for 36% of the total variation.

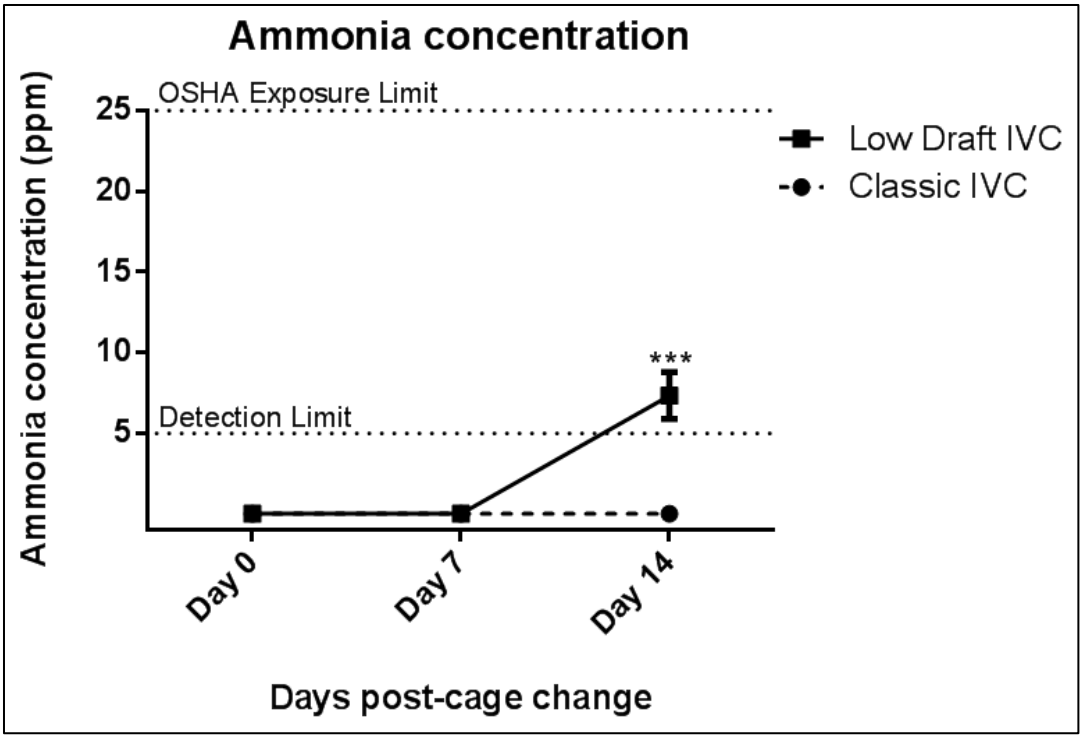


**Figure 4-5** Effect of novel, low draft IVC on micro-environment ammonia (n = 3 cages at stocking density 3). Error bars represent standard deviation. ***, $P < 0.001$

iv. **Discussion**

By day 14, the novel, low draft IVC had accumulated significantly higher ammonia than the classic IVC (Figure 4-5). This is not surprising given the *in silco* modeling showed a showed a substantial reduction in drafts directed towards the bedding. Drafts in contact with bedding have a desiccating effect that inhibits ammonia formation (Vogelweid *et al*., 2011), since cage moisture content is closely associated with ammonia production (Silverman *et al*., 2009). These results suggest there is a trade-off between shielding the animals from drafts (Figure 4-4) and ammonia concentrations (Figure 4-5).

Despite the higher concentration of ammonia, the 2-week cage change interval is appropriately maintained within the novel, low-draft IVC design. The ammonia

concentration of 7 ppm at day 14 post-cage change is substantially below the federally mandated human time-weight average exposure limit of 25 ppm (OSHA, 1997) and nearly an order of magnitude below the concentrations associated with respiratory and ocular lesions in mice (Vogelwied *et al.*, 2011).

By designing engineering controls that are compatible with current ventilated rack systems, reducing cold-stress in mice (Figure 4-4), and maintaining low ammonia concentrations (Figure 4-5), we speculate the benefits of the low-draft IVC will be cost-effective, scalable to large vivariums, and could be adopted rapidly. The design change only requires a fairly small alteration of the cage cover and no alteration in cage changing procedures. Without changing labor practices, ventilation equipment or the cage rack, this low cost engineering control can be readily adopted with minimal impact on vivarium operations.

# Chapter 5: Concluding Remarks

## I. What is the appropriate environmental temperature?

The right environmental temperature is the one that allows murine models to best model human conditions. Prospective studies of the translational success rate of rodent models based on murine thermal biology do not exist to our knowledge. Thus, the ideal temperature is unknown.

The option of maintaining mice at thermoneutral temperatures (if that is the ideal temperature for translational research) is impractical: the murine thermoneutral neutral zones span a very small range (1-3°C), varies greatly by metabolic state (e.g. obesity, pregnancy, lactation, etc.; Gordon, 2012), phenotype (e.g. hirsute and nude mice; David *et al.*, 2013a), disease state (e.g. cancer mediated cachexia; Tsoli *et al.*, 2012), time of day, and cage environment (Figure 1-2; Gordon, 2004; Gordon, 2012; David *et al.*, 2013a). The fluctuating and narrow thermoneutral zone of mice would make relying on environmental temperatures alone to support murine thermal biology impossible. In addition, raising the environmental temperature would cause staff discomfort and increase the costs of utilities.

## II. Other approaches to mitigating cold-stress

Other approaches to alleviating cold-stress in mice take advantage of the mouse's innate thermoregulatory behaviors such as social huddling (chapter 2), nest building (Gaskill *et al*, 2012), or shelter seeking (David *et al*., 2013b). Each of these approaches have been summarized in table 5-1:

| Table 5-1: Approaches to reducing cold-stress in the vivarium | | | |
|---|---|---|---|
| | Advantages | Disadvantages | Reference |
| Nesting material | Ablates thermotaxis, implying reduced cold-stress; inexpensive | Reduce visualization, difficult conduct health checks; increased cage change labor | Gaskill *et al.*, 2012; Gaskill *et al*., 2013 |
| Shelters | Ablates cold-stress associated with IVCs; inexpensive | Fixed objects associated with fighting in some male mice; possible increase in waste gas accumulation; increased cage change labor | David *et al.*, 2013b |
| Deep bedding | Maintains core body temperature | Increased husbandry costs, increased cage change labor; reduced visualization making it difficult to conduct health checks | Gordon, 2004 |
| Increased vivarium temperature | Reduced cold-stress, reduced cold-stress associated with drafts | Increased costs, staff discomfort; risks heat exhaustion in mice; increases cage ammonia; increase power consumption | David *et al.*, 2013a; Chappell and Holsclaw, 1984; Corning and Lipman 1991; NRC, 2010 |
| Independent HVAC conditioned air delivery to IVC | Conditioned, warm air can be delivered to mouse IVC separate from room air; staff comfort maintained | Expensive capital investment required plus ongoing utilities costs; must be included in building design or retrofitted at high costs | Clifton Roberts, DVM, ACLAM |
| IVC with heated air supply | Conditioned, warm air can be delivered to mouse IVC, separate from room air; human stuff comfort maintained | Expensive capital investment, only available with one vendor; not in production scale at the time of this publication; increased power consumption | Alterative Designs, Siloam Springs, AR |
| IVC designed to reduce drafts on mice | Mitigates cold-stress associated with IVC drafts; compatible with current capital equipment | Not commercially available; only addresses draft induced cold-stress | David and Stout, 2013 |

**Table 5-1** Summarizes major advantages and disadvantages of various approaches to mitigate cold-stress in mice. See references for detailed discussions.

## III. Impact on science

Regulatory bodies have very limited data to determine proper environment parameters. In the absence of performance data, regulatory bodies depend on professional judgment and murine behavioral data instead of scientific outcome metrics (Toth *et al.,* 2011; NRC, 2011). A wide variety of murine body systems and models of human disease are already known to be negatively impacted by chronic, mild cold-stress: cardiovascular, neuroendocrinology, metabolism, and oncology (Karp, 2012). The true impact of cold-stress on translational science is unknown; and further studies should be conducted, especially on the translational aspect, to determine the proper environmental conditions.

## IV. Recommendations

Until performance data describing the impact of housing conditions on translational research is available, we recommend the following husbandry practices: raise the environmental temperature to 23°C-25°C to minimize the metabolic consequences of drafts (Figure 3-2; Chappell and Holsclaw, 1984) without risking heat exhaustion (Gordon, 2012), minimizing drafts of IVCs via engineering controls (Chapter 4), maintaining a minimum of 3 mice per cage (Chapter 2), and allowing mice to behaviorally thermoregulate through shelters or nesting (David *et al*, 2013b; Gaskill *et al*, 2012). The amount of nesting material required to ablate thermotaxic behavior at specific environmental temperatures have been reported (Gaskill *et al*., 2012). Gaskill *et al*. recommends 8-10 grams of highly malleable material at “room temperatures” (2012). The amount of nesting material can be reduced with higher environmental temperatures (Gaskill *et al.*, 2012), potentially allowing health check observations while

simultaneously meeting the thermal regulatory needs of mice. In contrast, shelters can be made of red translucent polycarbonate or polyethylene plastics that facilitate health case observations. Moreover, these plastics are the same material as the cage, reducing the risk of unintended toxins introduction in the cage that has been associated with some nesting materials (Tischkau and Mukai, 2009).

Each of the recommended approaches are cumulative and utilizing the combination of these approaches will minimize the disadvantages of each technique (Table 5-1). Gordon observed mice behaviorally thermoregulate to minimize energy expenditure (2012). Placing mice in barren cages limits their behaviors, their preferred and primary murine thermoregulatory adaption (Gaskill *et al.*, 2013; Gaskill *et al.*, 2009; Gordon, 2012; Gordon, 1985). Promoting behavioral adaptions via nesting material or shelters will allow mice to titrate their thermal needs in proportion to the thermal stress they experience, which varies by metabolic state, phenotype, disease state, and caging environment. Mouse driven behavioral titration will be an improvement and more dynamic than relaying solely on environment temperature. We speculate that by facilitating behavioral titration of thermal environments, this will minimize the experiment variability between housing types (David *et al.*, 2013b), increase the reproducibility between institutions, and may lead to better models of human disease.

These recommendations should be revaluated when translational performance studies are available.

# REFERENCES

An XL, Zou JX, Wu RY, Yang Y, Tai FD, Zeng SY, Jia R, Zhang X, Liu EQ, Broders H. 2011. Strain and sex differences in anxiety-like and social behaviors in C57BL/6J and BALB/cJ mice. Experimental animals / Japanese Association for Laboratory Animal Science 60:111-123.

Anon. 2009. Troublesome variability in mouse studies. Nature neuroscience 12:1075.

Al-Hili F, Wright EA. 1983. The effects of changes in the environmental temperature on the growth of bone in the mouse: radiological and morphological study. Br. J Exp Pathol 64: 43-52.

Arakawa H, Blanchard DC, Blanchard RJ. 2007. Colony formation of C57BL/6J mice in visible burrow system: identification of eusocial behaviors in a background strain for genetic animal models of autism. Behav Brain Res 176(1): 27-39.

Atwater WO, Rosa EB. 1899. Description of new respiration calorimeter and experiments on the conservation of energy in the human body. USDA Bull 63, Washington, DC.

Baccan CG, Sesti-Costa R, Chedraoui-Silva S, Mantovani B. 2010. Effects of cold stress, corticosterone and catecholamines on phagocytosis in mice: differences between resting and activated macrophages. Neuroimmunomodulation 17: 379–385.

Batchelder P, Lynch CB, Schneider JE. 1982. The effects of age and experience on strain differences for nesting behavior in *Mus musculus*. Behav Genet 12(2): 149-59.

Bartelt A, Bruns OT, Reimer R, Hohenberg H, Ittrich H, Peldschus K, Kaul MG, Tromsdorf UI, Weller H, Waurisch C, Eychmuller A, Gordts PL, Rinninger F, Bruegelmann K, Freund B, Nielsen P, Merkel M, Heeren J. 2011. Brown adipose tissue activity controls triglyceride clearance. Nat Med 17(2): 200-5.

Baumans V, Schlingmann F, Vonck M, van Lith HA. 2002. Individually ventilated cages: beneficial for mice and men? Contemp Top Lab Anim Sci 41**:**13–19.

Brielmeier M, Mahabir E, Needham JR, Lengger C, Wilhelm P, Schmidt J. 2006. Microbiological monitoring of laboratory mice and biocontainment in individually ventilated cages: a field study. Lab Anim 40(3): 247-60.

Cannon B, Nedergaard J. 2010. Nonshivering thermogenesis and its adequate measurement in metabolic studies. J of Exp Bio 214: 242-53.

Celi FS. Brown adipose tissue-when it pays to be inefficient. N Engl J Med 360(15): 1553-6.

Chappell MA, Holsclaw DS. 1984. Effects of wind on thermoregulation and energy balance in deer mice (*Peromyscus maniculatus*). J Comp Physiol B 154: 619-625.

Commission for Thermal Physiology of the International Union of Physiological Sciences. 2001. Glossary of terms for thermal physiology. Jap J of Physiology 51(2): 245-280.

Compton SR, Homberger FR, MacArthur-Clark J. 2004. Microbiological monitoring in individually ventilated cage systems. Lab anim 33: 36-41.

Conger DL, Perazzo TM, d'Artenay MD. 2011. U.S. Patent 7,913,650 B2: Containment systems and components for animal husbandry. Washington, DC: U.S. Patent and Trademark Office.

Conley KE, Porter WP. Heat loss regulation: role of appendages and torso in the deer mosue and the white rabbit. J Comp Physiol B 155(4):423-31.

Corning BF, Lipman NS. 1991. A comparison of rodent caging systems based on microenvironmental parameters. Lab Anim Sci 41(5): 498-503.

Crabbe JC, Wahlsten D, Dudek BC. 1999. Genetics of mouse behavior: interactions with laboratory environment. Science, 284 (5420): 1670-2.

David JM, Chatziioannou AF, Taschereau R, Wang H, Stout DB. 2013a. The hidden cost of housing practices: using noninvasive imaging to quantify the metabolic demands of chronic cold stress of laboratory mice. Comp Med 63(5): 386-91.

David JM, Knowles S, Lamkin DM, Stout DB. 2013b. Individually ventilated cages impose cold stress on laboratory mice: a source of systemic experimental variability. J Am Assoc Lab Anim Sci 52(6): 738-44.

David JM, Stout DB. 2013c. U.S. 61,895,885 (provisional): Device, System, and Method for Measuring and Reducing Cold Stress of Housed Laboratory Animals. Washington, DC: U.S. Patent and Trademark Office.

DeRuisseau LR, Parsons AD, Overton JM. 2004. Adaptive thermogenesis is intact in B6 and A/J mice studied at thermoneutrality. Metabolism 53:1417–1423.

Doughman E. 2013. Cages prevalent in animal facilities, belief in global housing standards grows. Animal Lab News.

Ferrannini E. 1988. The theoretical bases of indirect calorimetry: a review. Metabolism 37(3): 287-301.

Foster DO, Frydman ML. 1979. Tissue distribution of cold-induced thermogenesis in conscious warm- or cold-acclimated rats reevaluated from changes in tissue blood flow: the dominant role of brown adipose tissue in the replacement of shivering by nonshivering thermogenesis. Can J Physiol Pharmacol 57(3): 257-70.

Fueger BJ, Czernin J, Hildebrandt I, Tran C, Halpern BS, Stout D, Phelps ME, Weber WA. 2006. Impact of animal handling on the results of $^{18}$F-FDG PET studies in mice. J Nucl Med 47:999–1006.

Gamble MR, Clough G. 1976. Ammonia build-up in animal boxes and its effect of rat tracheal epithelium. Lab Anim (10):93–104.

Garbiel GS, Campbell NE, Park CS, Murrary D, Irwin L, Gerringer R, Eldreth EK, Lastowski PA, Miller C, Minder. U.S. Patent 8,544,416: Ventilated rack system. Washington, DC: U.S. Patent and Trademark Office.

Gaskill BN, Rohr SA, Pajor EA, Lucas JR, Garner JP. 2009. Some like it hot: mouse temperature preference in laboratory housing. App An Behav Sci 116: 279-85.

Gaskill BN, Gordon CJ, Rajor EA, Lucas JR, Davis JK, Garner GP. 2012. Heat or Insulation: behavioral titration of mouse preference for warmth or access to a nest. PloS one 7(3): e32799.

Gaskill GN, Winnicker C, Garner JP, Pritcheet-Corning K. 2013. The naked truth: breeding performance in nude mice with and without nesting material. App An Behav Sci 143(2): 110-116.

Geiger R, Aron RH, Todhunter P. 2009. The climate near the ground. Landam (MA): Rowman and Littlefield Publishers.

Giard DJ. Aaronson SA, Todaro GJ, Arnstein P, Kersey JG, Dosik H, Parks WP. 1973. In vitro cultivation of human tumors: establishment of cell lines derived from a series of solid tumors. J Natl Cancer Inst 51: 1417-23.

Gilbert C, McCafferty D, Le Maho Y, Martrette JM, GIroud S, Blanc S, Ancel A. One for all and all for one: the energetic benefits of huddling in endotherms. Biol Rev Camb Philos Soc 85(3): 545-69.

Giralt M, Villarrova F. White, brown, beige/brite: different adipose for different functions? Endocrinology 154(9): 2992-3000.

Gordon CJ. 1985. Relationship between autonomic and behavioral thermoregulation in the mouse. Physiol Behav 34:687–690.

Gordon CJ. 1993. Temperature regulation in laboratory rodents. Cambridge University Press, New York.

Gordon CJ, Becker P, Ali JS. 1998. Behavioral thermoreglatory responses of single- and group-housed mice. Physiol Behav 65: 255-62.

Gordon CJ. 2004. Effect of cage bedding on temperature regulation and metabolism of group-housed female mice. Comp Med 54(1): 63-8.

Gordon CJ. 2012. Thermal physiology of laboratory mice: defining thermoneutrality. J of Thermal Bio 37: 654-85.

Hammel HT. 1995. Thermal properties of fur. Am J Physio 183: 369-82.

Harschaw C, Alberts JR. 2012. Group and individual regulation of physiology and behavior: a behavioral, thermographic, and acoustic study of mouse development. Physiol Behav 16(5): 670-82.

Harvey PW, Sutcliffe C. 2010. Adrenocortical hypertrophy: establishing cause and toxicological significance. J Appl Toxicol 30: 617-26.

*Hasenau* J, Baggs R, Kraus A. *1993*. Microenvironments in microisolation cages using BALB/c and CD-1 mice. Contemp. Topics Lab. Anim. Sci., 32, 11–16.

Hedmaier G. 1975. The influence of the social thermoregulation on the cold-adaptive growth of BAT in hairless and furred mice. Pfluggers Arch 355(3): 261-6.

Hoglund AU, Renstrom A. 2000. Evaluation of individually ventilated cage systems for laboratory rodents: cage environment and animal health aspects. Lab Anim 35: 51-7.

Hutchinson L. 2011. High drug attrition rates-where are we going wrong? Nature review, clinical oncology, 8: 189-190.

Jae-Jin J. 2002. WO 2,002,011,523 A: Cage for breeding experimental animals and individually ventilated apparatus for cage rack system. Gevena, Switzerland: World Intellectual Property Organization.

Jacoby RO, Fox JG, Davisson M. 2002. Biology and diseases of mice. *Laboratory Animal Medicine*, 2nd ed. American College of Laboratory Animal Medicine.

Kaiyala KJ, Morton GJ, Leroux BG, Oqimoto K, Wisse B, Schwartz MW. 2010. Identification of body fat mass as major determinant of metabolic rate in mice. Diabetes 59(7): 1657-66.

Kokolus KM, Caitano ML, Lee CT, Eng JW, Waight JD, Hylander BL, Secton S, Hong CC, Gordon CJ, Abrams SI, Repasky EA. 2013. Baseline tumor growth and immune control in laboratory mice are significantly influenced y subthermoneutral housing temperature. Proc Nathl Acad Sci USA 110(50): 20176-81.

Karp CL. 2012. Unstressing intemperate models: how cold-stress undermines mouse modeling. J Exp Med 6: 1069-74.

Koivisto A, Siamen D, Nedergaard J. 2000. Norepinephrine-induced sustained inward current in brown fat cells: alpha(1)-mediated by nonselective cation channels. Am J Physiol Endocrinol Meta 279(5): E963-77.

Krinke EJ. 2004. Chapter 9: normative histology of organ; The laboratory mouse. Academic Press, Chappell Hill, NC.

Lange K, Carson R. 1984. EM reconstruction alogrithms for emission and transmission tomography. J Comput Assist Tomogr 8(2): 306-16.

Leon LR, Gordon CJ, Helwig BG, Rufolo DM, Blaha MD. 2010. Thermoregulatory, behavior, and metabolic response to heatstroke in conscious mouse model. Am J Physio Regul Intger Comput Physiol 299: 241-8.

Lim S, Honek J, Xue Y, Seki T, Cao Z, andersson P, Yang X, Hoaka K, Cao Y. 2012. Cold-induced activation of brown adipose tissue and adipose angiogenesis in mice. Nat Protoc 7(3): 606-15.

Lipman NS. Isolator rodent caging systems (state of the art): a critical view. Contemp Top Lab Anim Sci 38(5): 9-17.

Lodhi IJ, Semenkovich CF. 2009. Why we should put clothes on mice. Cell metabolism (9):111-112.

Memarzedeh F. 1998. Ventilation design handbook on animal research facilities using static microisolators, volume I and II. Office of Research Services, National Institutes of Health. Bethesda, Maryland.

Memarzadeh F, Harrison PC, Riskowski GL, Henze T. 2004. Comparison of environment and mice in static and mechanically ventilated isolator cages with different air velocities and ventilation designs. Contemp Top Lab Anim Sci 43(1): 14-20.

McCafferty DJ. The value of infrared thermography for research on mammals: previous applications and future directions. Mammal Review 37(3): 207-23.

McDonald RB, Day C, Carlson K, Stern JS, Horwitz BA. 1989. Effect of age and gender on thermoregulation. Am J Physio 257: 700-4.

Milite G. 2008. The evolution of individually ventilated cages. Animal Lab News.

Morrison SF, Nakamura K, Madden CJ. 2008. Central control of thermogenesis in mammals. Exp Physiol 93: 773-97.

Muller B and Grossniklaus U. 2010. Model organisms-a historical perspective. J Preoteomics 73(11): 2054-63.

National Research Council, Institute for Laboratory Animal Research. 2011. Guide for the Care and Use of Laboratory Animal.

Nicklas W, Homberger FR, Illgen-Wilcke B, Jacobi K, Kraft V, Kunstyr I, Mahler M, Meyer H, Pohlmeyer-Esch G. 1999. Implications of infectious agents on results of animal experiment. Lab An 33(S1): 39-87.

Nguyen KD, Qiu Y, Cui X, Goh YP, Mwangi J, David T, Mukudan L, Brombacher F, Locksley RM, Chawla A. 2011. Aleternatively activated macrophages produce catecholamines to sustain adaptive thermogenesis. Nature 480(7375): 104-8.

Norton P, Horn S, Pellegrino JG, Perconti P. 2006. Infrared detectors and detector arrays. In: Bronzino JD, editor. Medical devices and systems. Boca Raton (FL): CRC Press.

Occupational Health and Safety Administration. 1997. Occupational health and safety in the care and use of research animals. National Academy Press. Washington, DC.

Olsson IA, Dahlborn K. 2002. Improving housing conditions for laboratory mice: a review of 'environmental enrichment. Lab An 36: 243-270.

Ootsuka Y, Menezes RC, Zaretsky DV, Alimoradian A, Hunt J, Steganidis A, Oldfield BJ, Blessing WW. 2009. Brown adipose tissue thermogenesis heats brain and body as part of the brain-coordinated ultradian vasic rest-activity cycle. Neuroscience 164: 849-61.

Oufara S, Barre H, Rouanet JL, Chatonnet J. 1987. Adaptation to extreme ambient temperatures in cold-acclimated gerbils and mice. Am J physiol. 253: 39-45.

Pennycuik PR. 1967. A comparison of the effects of variety of factors on the metabolic rate of the mouse. Aust J Exp Med Sci 45: 331-46.

Phelps ME. 2006. PET: physics, instrumentation, and scanners. Springer.

Philips PK, Heath JE. 1995. Dependency of surface temperature regulation on body size in terrestrial mammals. J Thermal boil 20: 281-9.

Pinheiro J, Bates D. 2000. Mixed-effects models in S and S-PLUS. Basel (Switzerland): Springer.

Purohit RC, McCoy MD. 1980. Thermography in the diagnosis of inflammatory processes in the horse. Am J Vet Res 41:1167–1174.

Rasmussen S, Miller MM, Filipski SB, Tolwani RJ. 2011. Cage change influence serum corticosterone and anxiety-like behaviors in the mouse. J Am Assoc Lab Anim Sci 50(4): 479-83.

Rauch JC, Hayward JS. 1969. Topography and vascularization of brown fat in a small nonhibernator (deer mouse, *Peromyscus maniulatus*). Can J of Zoo 47: 1301-14.

Reeb-Shitaker CK, Harrison DJ, Jones RB, Kacergis JB, Myers DD, Paigen B. 1999. Control strategies for aeroallergens in an animal facility. J Allergy Clin Immunol 103: 139-46.

Reynolds RP, Kinard WL, Degraff JJ, Leverage N, Norton JN. 2010. Noise in a laboratory animal facility from the human and mouse perspectives. J Am Assoc Lab Anim Sci 49(5): 592-7.

Richter SH, Garner GP, Auer C, Junert J, Wurbel H. 2011. Systematic variation improves reproducibility of animal experiments. Nature methods 7: 167-268.

Romanovsky AA, Kulchitsky VA, Simon CT, Sugimoto N. 1998. Methodology of fever research: why are polyphasic fevers often thought to be biphasic? Am J Physio 275: 332-338.

Rudaya AY, Steiner AA, Robbin JR, Dragic AS, Romanovsky AA. 2005. Thermoregulatory response to lipopolysaccharide in the mouse: dependence on the dose and ambient temperature. Am J of Physio 289: 1244-52.

Scholander PF, Hock R, Walters V, Johnson F, Lrving L. 1950 Heat regulation in some arctic and tropical mammals and birds. Biol. Bull. 99: 237-258.

Schulz TJ, Tseng YH. 2013. Brown adipose tissue: development, metabolism, and beyond. Biochem J 453(2): 167-78.

Seale P, bjork B, Yang W, Kajimura S, Chin S, Kuang S, Scime A, Devarakonda, Conroe HM, Erdjument-BRomage H, Tempst P, Rudnicki MA, Beier DR, Spiegelman BM. 2008. PRDM16 controls a brown fat/skeletal muscle switch. Nature 454(21): 961-8.

Serrat MA, King D, Lovejoy CO. 2008. Temperature regulates limb length in homotherms by directly modulating cartilage growth. PNASE 105: 19348-353.

Sealander, JA. 1952. The relationship of nest protection and huddling to survival of peromyscus at low temperature. Ecology 33:63-71.

Speakman JR, Ward S. 1998. Infrared thermography: principles and applications. Zoology 101:224-32.

Silverman J, Bays DW, Baker SP. 2009. Ammonia and carbon dioxide concentrations in disposable and reusable static mouse cages. Lab animal 38:16-23.

Sutton Gm, Ptitsyn AA, Floyd ZE, Yu G, Wu X, Hamel K, Shah FS, Centanni A, Eilertsen K, Kheterpal I, Newman S, Leonardi C, Freitas MA, Bunnell B, Gimble JM. 2012. Biological aging alters circadian mechanism in murine brown adipose tissue deposits. Age 35: 533-47.

Stark DM. 2001. Wire-bottom versus solid-bottom rodent caging issues important ot scientists and laboratory animal science specialists. Comtemp Topics Lab Anim Sci 40(6): 11-14.

Swoap SJ, LI C, Wess J, Parsons AD, Williams TD, Overton JM. 2008. Vagal tone dominates autonomic control of mouse heart rate at thermoneutrality. Am. J. Physiol. Heart Circ. Physiol. (294)1581–1588.

Swoap SJ, Overton JM, Garber G. 2004. Effect of ambient temperature on cardiovascular parameters in rats and mice: a comparative approach. Am J Physiol Regul Integr Comp Physiol 287:R391–R396.

Thornhil J, Halvorson I. 1990. Brown adipose tissue thermogenic responses of rats induced by central stimulation: effect of age and cold acclimation. J Physiol 426: 317-33.

Tischkau SA, Mukai M. 2009. Activation of aryl hydrocarbon receptor signaling by cotton balls used for environmental enrichment. J Am Assoc Lab Anim Sci 48(4): 357-62.

Toth LA, Kregel K, Leon L, Musch LI. 2011. Environmental enrichment of laboratory rodents: the answer depends on the question. Comp Med 61(4): 614-21.

Tsoli M, Moore M, Burg D, Painter A, Taylor R, Lockie SH, Turner N, Warren A, Cooney G, Oldfield B, Clarker S, Roberston G. 2012. Activation of thermogenesis in brown adipose tissue and dysregulated lipid metabolism associated with cancer cachexia in mice. Cancer Res 72(17): 4373-82.

van der Veen DR, Shao J, Chapman S, Leevy WM, Duffield GE. 2012. A diurnal rhythm in glucose uptake in brown adipose tissue revealed by in vivo PET-FDG imaging. Obesity 20:1527–1529.

Vogelweid CM, Zapien KA, Honigford MJ, Li L, Li H, Marshall H. 2011. Effects of a 28-day cage-change interval on intracage ammonia levels, nasal histology, and perceived welfare of CD1 mice. J Am Ass of Lab Anim Sci 50:868-878.

Wang H, Stout DB, Chatziioannou AF. 2012a. Mouse atlas registration with nontomographic imaging modalities—a pilot study based on simulation. Mol Imaging Biol 14:408–419.

Wang H, Stout DB, Taschereau R, Gu Z, Vu NT, Prout DL, Chatziioannou AF. 2012b. MARS: a mouse atlas registration system based on a planar X-ray projector and an optical camera. Phys Med Biol 57:6063–6077.

Weibe WH. 1984. The thermoregulation of the nude mouse. Exp Cell Biol 52: 140-144.

Williams TD, Chambers JB, Henderson RP, Rashotte ME, Overton JM. 2002. Cardiovascular responses to caloric restriction and thermoneutrality in C57BL/6J mice. Am J Physiol Regul Integr Comp Physiol 282:R1459–R1467.